



UNIVERSITY OF
KWAZULU-NATAL

INYUVESI
YAKWAZULU-NATALI

*Fumonisin B₁ induced Antioxidant Response
in C57BL/6 Male Mice Brain*

By

Thabani Sibiya

B. Sc. B. Med. Sc. (Hons) (UKZN)

Submitted in fulfilment of the requirements for the degree of MMedSci. in

the Discipline of

Medical Biochemistry and Chemical Pathology

School of Laboratory Medicine and Medical Sciences

College of Health Sciences

Durban

2018

DECLARATION

This dissertation represents the original work by the author and has not been submitted in any form to another university. The work of others has been duly acknowledged in the text.

The research described in this study was carried out in the Discipline of Medical Biochemistry, School of Laboratory Medicine and Medical Science, College of Health Sciences, University of Kwa-Zulu Natal, under the supervision of Professor A.A. Chuturgoon, Dr S. Nagiah and Ms. T. Ghazi.

Mr. Thabani Sibiya

Date

ACKNOWLEDGEMENTS

My family

Rest in peace to my parents (Thembinkosi and Busisiwe), I am grateful to be your son and I hope you are proud of my progress in life. RIP gogo maShezi, gogo maNzaba, my sister Phumuzile, I love you all. To all my family members I appreciate everything that you have done for me, your continuous encouragement, support and patience is deeply appreciated.

Prof Anil Chuturgoon

Thank you for the opportunity to not only grow as a scientist but to be inspired and motivated. Although my genetic make-up will not allow me to be as tall as you, I wish God gives me the power to be a great man to this world as you. I will always be grateful to you for your guidance, support and encouragement.

Dr Savania Nagiah

Thank you for all your patience, advice, corrections, suggestions and contributions that enabled me to complete this dissertation and become a better scientist.

Miss Terisha Ghazi

I cannot thank you enough for all your patience, advice, corrections, suggestions, contributions to this dissertation and encouragement during difficult times. I am grateful for your presence throughout my study and making me a better scientist.

Miss Thilona Arumugam, Miss Taskeen Fathima Docrat and Mr. Naeem Sheik-Abdul

Thank you for all your assistance in and out of laboratory.

Fellow Master Students (2018)

Thank you, Lerise A. Peters for your friendship and encouragement, you are the best. Thank you Miss Sindi Nzima for your jokes.

National Research Foundation (NRF) and College of Health Sciences (CHS-UKZN)

I would like to thank NRF and CHS (UKZN) for scholarships and funding.

PRESENTATIONS

First presentation:

Fumonisin B1 induced Antioxidant Response in C57BL/6 Male Mice Brain

Sibiya, T., Nagiah, S., Ghazi, T., Chuturgoon, A.A.

School of Laboratory Medicine and Medical Sciences Research Symposium (29 August 2018),
University of Kwa-Zulu Natal, Durban, South Africa – Oral Presentation, Masters Students Category

Second presentation:

Fumonisin B1 induced Antioxidant Response in C57BL/6 Male Mice Brain

Sibiya, T., Nagiah, S., Ghazi, T., Chuturgoon, A.A.

College of Health Sciences Research Symposium (11th – 12th October 2018), University of Kwa-Zulu
Natal, Durban, South Africa – Oral Presentation, Masters Students Category

ABBREVIATIONS

AD	Alzheimer's disease
AO	Anti-oxidants
APS	Ammonium persulphate
ARE	Anti-oxidant Response Element
ATP	Adenosine triphosphate
BSA	Bovine serum albumin
CAT	Catalase
cDNA	Complementary deoxyribonucleic acid
CNS	Central nervous system
Cu	Copper
Cu¹⁺	Cuprous ions
Cu²⁺	Cupric ions
Cul3	Cullin 3
DNA	Deoxyribonucleic acid
dNTPs	Deoxynucleoside triphosphates
ELEM	Equine leukoencephalomalacia
ERK	Extracellular signal- regulated kinases
EpRE	Electrophile Responsive Element
ETC	Electron transport chain
FB₁	Fumonisin B ₁
FB₂	Fumonisin B ₂
FB₃	Fumonisin B ₃
Fe	Iron
fNrf2	Free floating Nrf2
GPx	Glutathione peroxidase
GSH	Glutathione (Reduced)
GST	Glutathione-s-transferase
hrs	Hours

H₂O	Water
H₂O₂	Hydrogen peroxide
H₃PO₄	Phosphoric acid
HCl	Hydrogen chloride
HO-1	heme oxygenase-1
HOCl	Hypochlorous acid
HRP	Horse radish peroxidase
IARC	International Agency for Research on Cancer
Keap-1	Kelch-like ECH associated protein 1
kNrf2	Keap1-binding Nrf2
LONP1	Lon-protease 1
min	Minute
MnSOD	Manganese-dependent superoxide dismutase
mRNA	Messenger ribonucleic acid
mtDNA	Mitochondrial deoxyribonucleic acid
NAD⁺	Nicotinamide adenine dinucleotide
NADPH	Nicotinamide adenine dinucleotide phosphate
Neh2	Nrf2-ECH homolog h2
NQO-1	NADPH-quinone oxidase
Nrf2	Nuclear-factor-erythroid 2 p45-related factor 2
NTD	Neuronal tube defects
ORF	Open Reading Frame
O₂	Oxygen
O₂^{•-}	Superoxide radicals
OGG1	8-Oxoguanine glycosylase
OH	Hydroxyl
PBMC	Peripheral blood mononuclear cells
PBS	Phosphate buffered saline
PCR	Polymerase chain reaction
PKC	Protein kinase C
pNrf2	Phosphorylated nuclear-factor-erythroid 2 p45- related factor 2
qPCR	Quantitative polymerase chain reaction
RBD	Relative band density

RFC	Relative fold change
RISC	RNA-induced silencing complex
ROS	Reactive oxygen species
RT	Room temperature
Sa	sphinganine
SDS	Sodium dodecyl sulphate
SDS-PAGE	Sodium dodecyl sulphate–polyacrylamide gel electrophoresis
SIRT 3	Sirtuin 3
SOD2	Superoxide dismutase 2
So	sphingosine
TCA	Tricarboxylic acid
Tfam	Mitochondrial transcription factor A
TMED	Tetramethylethylenediamine
TTBS	Tween 20-Tris buffered saline
Ub	Ubiquitination

LIST OF FIGURES

CHAPTER 2: LITERATURE REVIEW

Figure 2.1.	Chemical structures of some of the commonly produced mycotoxins (Malhotra, Srivastava et al. 2014).	4
Figure 2.2.	Structures and absolute configuration of fumonisin B ₁ (FB ₁), fumonisin B ₂ (FB ₂), fumonisin B ₃ (FB ₃), hydrolysed fumonisin B ₁ (HFB ₁), hydroxyed fumonisin B ₂ (HFB ₂), N-(carboxymethyl)-fumonisin B ₁ (NCM-FB ₁), N-(1-deoxy-Dfructos-1-yl) fumonisin B ₁ (NDF-FB ₁), Derythro-sphinganine (SA) and D-erythrospingosine (SO) (Humpf and Voss 2004).	6
Figure 2.3.	Structure of fumonisin B ₁ (Merrill, Van Echten et al. 1993).	7
Figure 2.4.	FB ₁ disruption of sphingolipid metabolism (prepared by author).	8
Figure 2.5.	Proposed model of Nrf2-mediated redox signalling. Ubiquitination (Ub); free floating Nrf2 (fNrf2); Keap1-binding Nrf2 (kNrf2) (Li and Kong 2009).	13
Figure 2.6.	Radical scavenging activity of SOD, CAT, and GPx, starting from SIRT-3 (Prepared by author).	14
Figure 2.7.	MiRNA biosynthesis and function (He and Hannon 2004). microRNA (miRNA); pri-microRNA (pri-miRNA); interfering RNA (siRNA)duplexes; RNA-induced silencing complex (RISC); open reading frame (ORF) (He and Hannon 2004).	16

CHAPTER 3: METHOD AND MATERIALS

Figure 3.1.	Animal treatment and brain extraction (Prepared by Author).	19
Figure 3.2.	Presentation of the BCA assay principle (prepared by author).	21
Figure 3.3.	Equipment used to prepare SDS-PAGE gels (Prepared by author)	22

Figure 3.4.	Immunoblotting and protein detection (Prepared by author)	25
Figure 3.5.	The steps of one PCR cycle leading up to DNA amplification (Prepared by author).	27
Figure 3.6.	Fluorescence increases drastically when dye molecules bind to dsDNA (Prepared by author)	28

CHAPTER 4: RESULTS

Figure 4.1.	(A)Protein expression of Nrf2 (24hrs: * $p=0,0144$; 10 days: ** $p=0,0094$), (B) Protein expression of pNrf2 (24hrs: * $p=0,0132$; 10 days: * $p=0,0462$) in mice brain exposed to FB ₁ .	32
Figure 4.2.	Protein expression of Catalase in mice brain exposed to FB ₁ for 24hrs ($p=0,1206$) and 10 days (** $p=0,0010$).	33
Figure 4.3.	mRNA levels of <i>Nrf2</i> in C57BL/6 mice brain exposed to FB ₁ for 24hrs (** $p=0,0001$) and 10 days (** $p=0,0013$).	34
Figure 4.4.	<i>MiR-141</i> expression in C57BL/6 mice brain exposed to FB ₁ for 24 hrs (** $p=0,0019$) and 10 days (** $p=0,0004$).	35
Figure 4.5.	mRNA levels of <i>SOD2</i> in C57BL/6 mice brain exposed to FB ₁ for 24 hrs (** $p=0,0070$) and 10 days ($p=0,2725$).	36
Figure 4.6.	mRNA levels of <i>GPx</i> in C57BL/6 mice brain exposed to FB ₁ for 24 hrs (** $p=0,0001$) and 10 days (** $p=0,0024$).	37
Figure 4.7.	mRNA levels of <i>Tfam</i> in C57BL/6 mice brain exposed to FB ₁ for 24 hrs (** $p=0,0003$) and 10 days (* $p=0,0196$).	38
Figure 4.8.	mRNA levels of <i>LONP1</i> in C57BL/6 mice brain exposed to FB ₁ for 24 hrs (** $p=0,0005$) and 10 days (* $p=0,0117$).	39

Figure 4.9. mRNA levels of *SIRT3* in C57BL/6 mice brain exposed to FB₁ for 24 hrs ($p= 0,0594$) and 10 days ($*p= 0,0283$). **40**

Figure 4.10. mRNA levels of *Tau* in C57BL/6 mice brain exposed to FB₁ for 24 hrs ($**p= 0,0054$) and 10 days ($*p= 0,0273$). **41**

APPENDIX A

Figure 6 mRNA levels of *NGO1* (24hrs: $**p= 0,0080$; 10 days: $p= 0,1292$) in mice brain exposed to FB₁. **57**

APPENDIX B

Figure 7 mRNA levels of *HO1* (24hrs: $***p= < 0.0001$; 10 days: $***p= < 0.0001$) in mice brain exposed to FB₁. **58**

APPENDIX C

Figure 8 *MiR-200a* expression in C57BL/6 mice brain exposed to FB₁ for 24 hrs ($***p < 0.0001$) and 10 days ($**p= 0,0051$). **59**

APPENDIX D

Figure 9 Standard curve displaying known concentrations of bovine serum albumin (BSA) used to determine the concentration of protein present in each sample **60**

LIST OF TABLES

CHAPTER 2: LITERATURE REVIEW

Table 2.1.	Mycotoxins, associated fungi, and food/feed crops at risk of contamination (Wu, Groopman et al. 2014).	5
-------------------	--	----------

CHAPTER 3: METHOD AND MATERIALS

Table 3.1.	Antibodies and the antibody dilutions used in western blotting.	24
Table 3.2.	The annealing temperatures and primer sequences for the genes of interest.	30

Table of Contents

DECLARATION.....	i
ACKNOWLEDGEMENTS	ii
PRESENTATIONS.....	iii
ABBREVIATIONS	iv
LIST OF FIGURES	vii
LIST OF TABLES	x
ABSTRACT.....	xiii
Chapter 1 – Introduction.....	1
Chapter 2 - Literature Review	4
2.1 Mycotoxins.....	4
2.1.1 <i>Fumonisin</i>	5
2.1.2 <i>Fumonisin B₁</i>	7
2.1.3 <i>Structure of FB₁</i>	7
2.1.4 <i>Mechanism of action</i>	8
2.1.5 <i>Molecular Toxicity</i>	10
2.2 Neurotoxicity	11
2.3 Oxidative Stress.....	11
2.4 Antioxidant response	12
2.5 miRNA	16
2.6 Oxidative stress-induced diseases in the brain	17
Chapter 3 - Materials and Methods	18
3.1 Materials.....	18
3.2 Animal Treatment.....	18
3.3 Protein expression – western blot.....	19
3.4 Protein Isolation.....	20
3.5 Protein quantification and standardization.....	20
3.6 Sodium dodecyl sulphate–polyacrylamide gel electrophoresis (SDS-PAGE) and Western Blotting.....	22
3.7 Gene expression – Quantitative polymerase chain reaction	25
3.8 Statistical Analyses.....	31
Chapter 4 – Results.....	32
4.1 Western Blot.....	32
4.1.1 <i>Antioxidant response</i>	32
4.1.2 <i>Detoxification of peroxides</i>	33

4.2 Quantitative polymerase chain reaction (qPCR)	34
4.2.1 Antioxidant response	34
4.2.2 Post transcriptional regulation of Nrf2	35
4.2.2 Superoxide detoxification	36
4.2.3 Detoxification of peroxides	37
4.2.4 Mitochondrial stress response	38
4.2.5 Expression of neuronal disease related genes	41
Chapter 5 – Discussion	42
5.1 Limitations and Future studies	45
5.2 Conclusion	45
References	45
APPENDIX A	57
APPENDIX B	58
APPENDIX C	59
APPENDIX D	60

ABSTRACT

Background: Fumonisin B₁ (FB₁), a mycotoxin produced by the *Fusarium* species, contaminates maize. In South Africa maize is a dietary staple and FB₁ endangers human and animal health. FB₁ is known to have neurodegenerative effects; inhibits mitochondrial respiration, causes mitochondrial membrane depolarization and excessive ROS production. This study investigated the antioxidant response in mice brain after acute (24 hrs) and prolonged (10 days) exposure to FB₁.

Methods: Four groups (Control acute, FB₁ acute, Control prolonged, FB₁ prolonged) of C57BL/6 male mice (n=5 per group) were used. All controls were orally administered 0.1M PBS and FB₁ groups were administered 5mg/kg of FB₁. Following acute and prolonged exposure, the mice were euthanised by halothane anaesthesia. Brain tissues were harvested and stored in Qiazol and Cytobuster for RNA and protein isolation, respectively. Protein expression of CAT, pNrf2 and Nrf2 were determined using western blots. The mRNA expression of *Nrf2*, miR-141, *SOD2*, *GPx*, *Tfam*, *LON*, *SIRT3* and *Tau* were determined using qPCR.

Results: Protein expression of Nrf2 (Acute: **p*=0,0144; prolonged: ***p*=0,0094) and pNrf2 (acute: **p*=0,0132; prolonged: **p*=0,0462) was significantly increased upon 24 hrs and significantly decreased upon 10 days in tissue exposed to FB₁, while mRNA levels of *Nrf2* were significantly reduced upon acute (***p*=0,0001) and prolonged (***p*=0,0013) exposure. FB₁ induced a significant decrease in miR-141 levels in tissue following acute (***p*=0,0019) and prolonged (***p*=0,0004) exposure. FB₁ increased the protein expression of CAT in tissue following acute (*p*=0,1206) and significantly increased expression upon prolonged (***p*=0,0010) exposure. FB₁ also significantly increased the mRNA expression of *GPx* in acute (***p*=0,0001) and prolonged (***p*=0,0024) exposure. FB₁ significantly decreased the expression of *SOD2* in mice brain following acute (***p*=0,0070) and non-significantly decrease upon prolonged (*p*=0,2725) exposure. *Tfam* and *LONP1* levels were significantly decreased upon acute (***p*=0,0003, ***p*=0,0005) and prolonged (**p*=0,0196, **p*=0,0117) exposure to FB₁ respectively. However, *SIRT3* expression was decreased upon acute (*p*=0,0594) and significantly increased upon prolonged (**p*=0,0283) exposure to FB₁. The mRNA expression of *tau* was significantly reduced upon acute (***p*=0,0054) and prolonged (**p*=0,0273) exposure to FB₁.

Conclusion: FB₁ compromises antioxidant and mitochondrial survival responses in mice brain. This may have implications in FB₁-induced neurodegeneration.

Chapter 1 – Introduction

Fumonisin B₁ (FB₁) is a type 2B carcinogenic mycotoxin product of ubiquitous soil fungi, *Fusarium verticilloides* and *Fusarium proliferatum*. It occurs worldwide as a contaminant of maize and maize products (Marasas 2001). In South African communities where maize is a staple food source, FB₁ poses a serious threat to human and animal health since it is resistant to food processing methods (Scott 2012). FB₁ has been linked to oesophageal cancer, primary liver cancer and neural tube defects among communities where maize is a staple food (Detrait, George et al. 2005). It is also one of the most recognized mycotoxins derived from *F. verticilloides* that has neurodegenerative effects (Domijan and Abramov 2011).

FB₁ can pass through the blood-brain barrier due to its high polarity and small size (Bezuidenhout, Gelderblom et al. 1988). The most known neurological disorder caused by exposure to fumonisins is equine leukoencephalomalacia (ELEM) (Brownie and Cullen 1987). Consumption of fumonisins is also linked with the aetiology of neuronal tube defects (NTD) in children (Marasas, Riley et al. 2004). The neurotoxic effects of FB₁ are associated with decreased activity of glial cells (Kwon, Slikker Jr et al. 2000), inhibition of axonal growth (Harel and Futerman 1993), impaired myelin formation and deposition and delayed oligodendrocyte maturation (Monnet-Tschudi, Zurich et al. 1999). Furthermore, FB₁ has demonstrated inhibition of *de novo* ceramide synthesis, stimulation of astrocytes, and upregulation of pro-inflammatory cytokines in murine brain (Osuchowski, Edwards et al. 2005).

On a molecular level, FB₁ is known to disrupt sphingolipid metabolism in many animal species, including mice (Martinova and Merrill 1995), rats (Riley, Hinton et al. 1994), pigs (Riley, An et al. 1993), and horses (Wang, Ross et al. 1992, Riley, Showker et al. 1997). Due to FB₁ structural similarity to sphingoid bases, it interferes with sphingolipid metabolism, leading to cytotoxicity and carcinogenicity (Riley, Enongene et al. 2001). Oxidative stress has also been identified as a molecular mechanism of FB₁ neurotoxicity (Stockmann-Juvala, Mikkola et al. 2004). The ability of FB₁ to elevate reactive oxygen species (ROS) is rather a consequence rather than a mechanism of its toxicity. FB₁ inhibits mitochondrial complex I of the electron transport chain (ETC), decreasing the rate of mitochondrial and cellular respiration, increasing mitochondrial membrane depolarization and induction of mitochondrial ROS production (Domijan and Abramov 2011).

Altered redox homeostasis has massive implications for neurological health, with oxidative damage being a common pathological mechanism in multiple neurodegenerative disorders. Cellular redox control is mediated by Nuclear-factor-erythroid 2 p45-Related Factor 2 (Nrf2) (López-Alarcón and Denicola 2013). Binding of Nrf2 to the antioxidant response element (ARE) leads to induction and expression of cytoprotective enzymes like glutathione S-transferase (GST), superoxide dismutase (SOD), heme oxygenase-1 (HO-1) and NADPH-quinone oxidase (NQO-1) (Eggler, Gay et al. 2008).

The presence of electrophiles and ROS activates detoxifying and antioxidant genes (Buetler, Gallagher et al. 1995, Hayes and Pulford 1995, Itoh, Wakabayashi et al. 2003). Disruption or inhibition of Nrf2 has implications for cellular antioxidant response and overall health. As a consequence, Nrf2 has become a prime target in maintaining neurological function.

The stability and cellular distribution of Nrf2 is tightly controlled by its inhibitory binding protein Kelch-like ECH-associated protein 1 (Keap1) (Itoh, Wakabayashi et al. 1999, Nguyen, Nioi et al. 2009, Huang, Li et al. 2015). The main role of Nrf2-Keap1 system is the regulation of cellular defence against environmental insults (Ishii, Itoh et al. 2000). Keap1 represses Nrf2 transactivation activity (Itoh, Wakabayashi et al. 1999); however, during Nrf2-signalling, the Nrf2/Keap1 complex is dissociated in the cytoplasm and Nrf2 translocates to the nucleus where it binds to the ARE and initiates the transcription of cytoprotective enzymes (Hansen, Watson et al. 2004).

Nrf2 expression can be altered by increased free radicals or the activity of other regulatory proteins. Epigenetic regulation of Nrf2 provides a scarcely described mechanism of regulation. MicroRNAs (miRNAs) are a group of endogenous, small (18 to 25 nucleotides), noncoding RNAs that post-transcriptionally regulate gene expression by base sequence recognition (Chen, Xu et al. 2014). MicroRNA-141 (miR-141) is involved in negatively regulating the expression of Keap1 and thus influences Nrf2 signalling (Eades, Yang et al. 2011).

Considering the diverse function of Nrf2 in cellular defence and survival, establishing the role of this protein in FB₁ induced neurotoxicity may provide a novel mechanism of FB₁ toxicity. Furthermore, evaluating regulatory proteins or miRNA that control this pathway can uncover targeted therapeutic interventions.

1.1 Aim & Objectives

The aim of this study was to investigate the acute (24 hr) and prolonged (10 days) effects of FB₁ on the Nrf2 antioxidant pathway in C57BL/6 male mice brain. It was hypothesized that FB₁ altered redox homeostasis in the brain, thus affecting Nrf2-mediated antioxidant signalling and mitochondrial stress response.

The objectives of this study:

- To determine the effects of FB₁ on phospho-Nrf2(S40) levels and Nrf2 protein expression in mouse brain at 24 hrs and 10 days

- To determine the effects of FB₁ on the mRNA levels of *Nrf2* in mice brain at 24 hrs and 10 days
- To investigate Nrf2-regulated antioxidant genes such as *SOD2*, *SIRT3* and *GPx* in mice brain upon acute(24hr) and prolonged (10 days) exposure to FB₁
- To evaluate mitochondrial stress response markers in mice brain upon acute(24hr) and prolonged (10 days) exposure to FB₁
- To investigate the effect of FB₁ on the epigenetic modulation of Nrf2 by miR-141 in mice brain upon acute (24 hr) and prolonged (10 days) exposure

Research Questions:

- Does FB₁ alter Nrf2 and downstream targets in mice brain?
- Does FB₁ alter miR-141 expression in mice brain?
- Does FB₁ induce different Nrf2-mediated antioxidant response following acute and prolonged exposure?

Chapter 2 - Literature Review

2.1 Mycotoxins

Mycotoxins, products of filamentous fungi, produced as secondary metabolites and can be toxic to humans and animals (da Rocha, Freire et al. 2014). Several fungal species can produce the same mycotoxin (Hussein and Brasel 2001). They are produced inclusively as the fungus reaches maturity, and they vary in size and shape, from just heterocyclic rings of up to fifty Dalton in molecular weights, to groups with molecular weight of greater than five hundreds Dalton in total with six to eight heterocyclic rings arranged unevenly (Figure 1) (da Rocha, Freire et al. 2014). These mycotoxins contaminate foods and feeds such as nuts, corn, rice, and cereals. This contamination can take place during growth and harvest in the fields as well during storage (da Rocha, Freire et al. 2014).

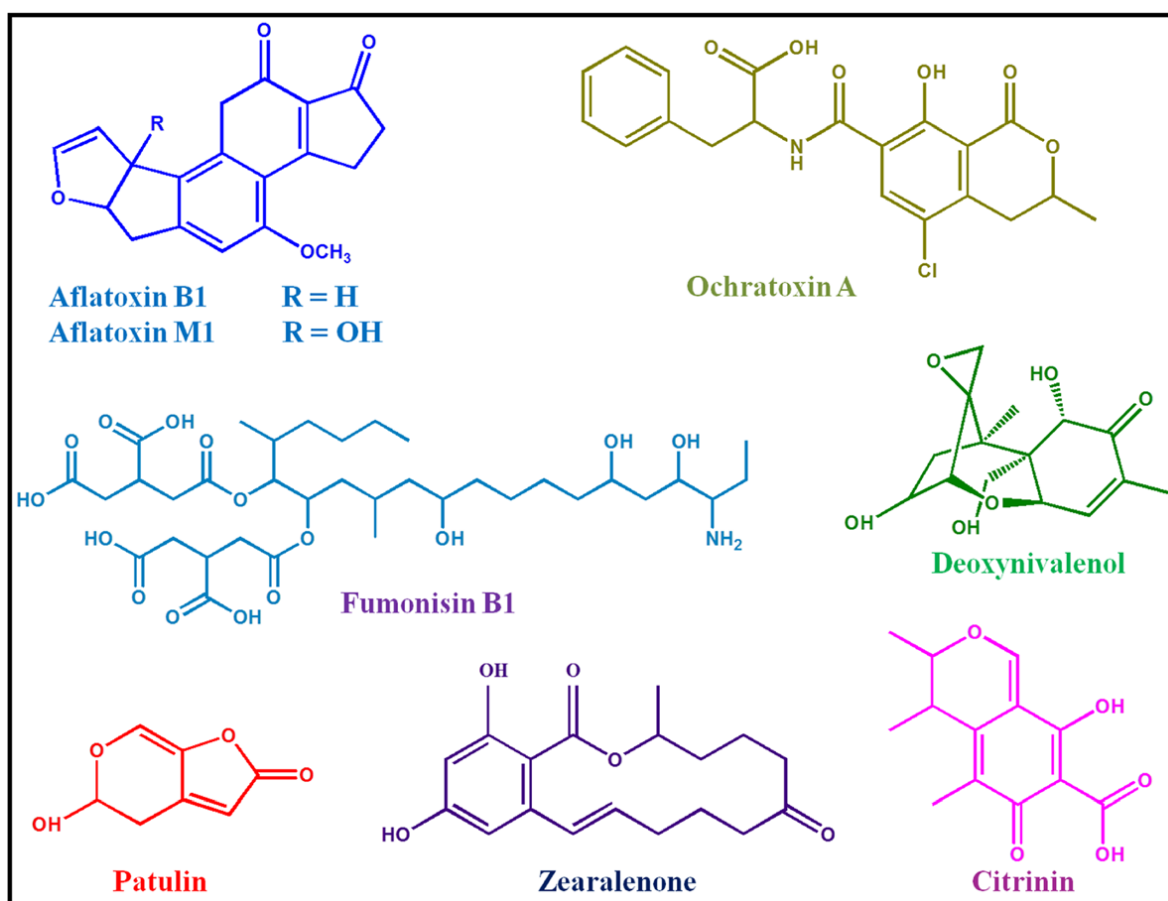


Figure 2.1: Chemical structures of some of the commonly produced mycotoxins (Malhotra, Srivastava et al. 2014).

Humans and animals are exposed to mycotoxins via direct or indirect contamination (Smith, Solomons et al. 1995). Humans can ingest mycotoxins through eating contaminated plant products and food derivatives from products such as milk, cheese, and meat (Smith, Solomons et al. 1995). Mycotoxins

exert several toxic effects on humans and animals including carcinogenicity, genotoxicity, teratogenicity, nephrotoxicity, hepatotoxicity, reproductive disorders, and immune suppression (Galvano, Piva et al. 2001).

The mycotoxins that are of major public health interest are aflatoxins, fumonisins, trichothecenes, and ochratoxin A (Table 2.1) (Wu, Groopman et al. 2014). These mycotoxin are primary products of fungi of the genera *Aspergillus*, *Fusarium*, and *Penicillium*, which are common contaminants of food crops (Wu, Groopman et al. 2014).

Table 2.1: Mycotoxins, Producing fungi, and Associated food/feed crops contaminated (Wu, Groopman et al. 2014).

Mycotoxin	Producing fungi	Associated food/feed crops
Aflatoxins	<i>Aspergillus flavus</i> <i>A. parasiticus</i>	Maize, peanuts, tree nuts, copra, spices, cottonseed
Fumonisin	<i>Fusarium verticillioides</i> <i>F. proliferatum</i> <i>A. niger</i>	Maize
Trichothecene mycotoxins	<i>F. graminearum</i> <i>F. culmorum</i>	Maize, wheat, barley, oats
Ochratoxin A	<i>Penicillium verrucosum</i> <i>A. ochraceus</i> <i>A. carbonarius</i> <i>A. niger</i>	Maize, wheat, barley, oats, dried meats and fruits, coffee, wine

2.1.1 Fumonisin

Fumonisin are divided into 28 analogues and are categorized as A, B, C and P. Fumonisin B (FB) is divided into 4 groups i.e. FB₁, FB₂, FB₃, FB₄ (Bezuidenhout, Gelderblom et al. 1988, Musser and Plattner 1997, Seo and Lee 1999, Omurtag 2008). They are products of numerous *Fusarium* species, primarily *F. verticillioides*, *F. proliferatum* and *F. anthophilum*. Fumonisin have been studied and found to be a contaminant of maize, rice, sorghum, beans and wheat. Approximately over 60% of all maize and maize based products are contaminated by fumonisin, which is unfortunate since maize is a staple food source to most African and South African communities (Omurtag 2008). FB₁ is the most predominant and more toxic than FB₂ and FB₃ (Humpf and Voss 2004, Omurtag 2008).

Fumonisin isomers are diesters of propane-1,2,3-tricarboxylic acid (TCA) and similar long-chain aminopolyol backbones, but FB₁ is a 2S-amino-12S,16R-dimethyl-3S,5R,10R,14S,15R-pentahydroxyeicosane. It is also noteworthy that fumonisins have resemblance in structure with sphingoid bases sphinganine (SA) and sphingosine (SO) with TCA groups added at the C-14 and C-15 positions (Figure 2.2) (Humpf and Voss 2004). FB₂ and FB₃ are distinct from FB₁ by the absence of the hydroxyl group at C-1 for FB₂ and C-5 for FB₃, respectively. In addition, C-5 and C-10 hydroxyl groups are absent in FB₄ (Humpf and Voss 2004, Krska, Welzig et al. 2007).

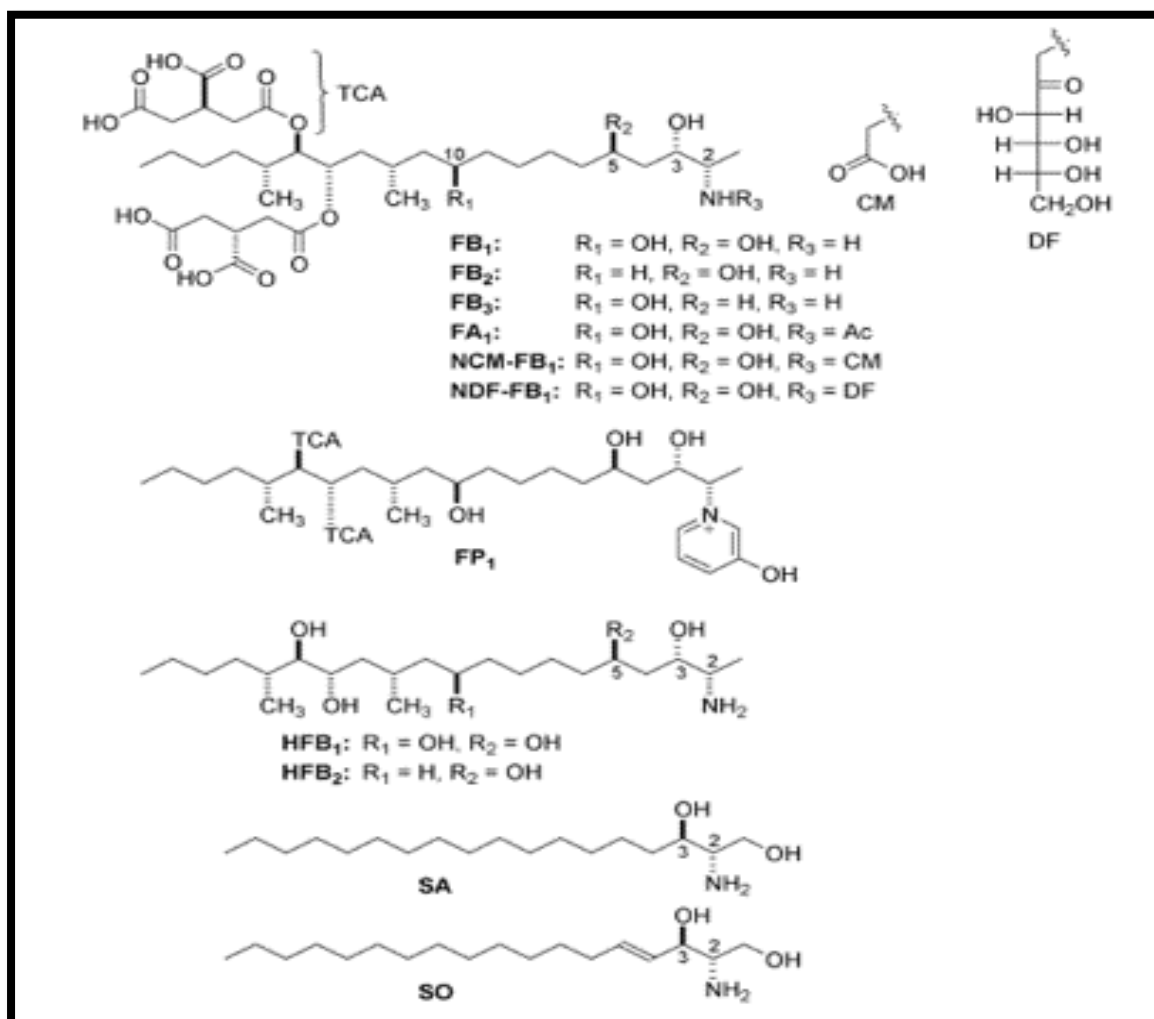


Figure 2.2: Structures and complete conformation of fumonisin B (FB) (Humpf and Voss 2004).

Fumonisin was first isolated from cultures of *F. verticilloides* or *F. moniliforme* strain MRC 826 in South Africa in 1988 (Gelderblom, Jaskiewicz et al. 1988). The isolated material of *F. moniliforme* MRC 826 from maize intended for human consumption in South Africa's Transkei region was found to cause ELEM in horses (Kriek, Kellerman et al. 1981). Several studies then linked FB₁ with the high incidence of oesophageal cancer, primary liver cancer and neural tube defects among communities where maize is a staple food (Detrait, George et al. 2005). FB₁ was reported to fall under a class of

group 2B carcinogens by the International Agency for Research on Cancer (IARC) (Domijan and Abramov 2011).

2.1.2 Fumonisin B₁

Fumonisin B₁ (FB₁) is one of the most recognized mycotoxins produced by *F. verticilloides* mould (Domijan and Abramov 2011). FB₁ is heat-stable and cannot be destroyed by normal industrial processing or cooking (Creppy 2002, Scott 2012). This is of particular concern in developing countries with hot and humid climates that promote fungal growth. Fumonisin initially gained notoriety when it was associated with oesophageal cancer in communities where home-grown maize is a staple food such as in Transkei (South Africa), China and North Eastern Italy (Rheeder, Marasas et al. 1992, Thiel, Marasas et al. 1992, Peraica, Radić et al. 1999).

FB₁ is a highly polar mycotoxin enabling it to traverse cellular membranes thus enhancing toxicity (Bezuidenhout, Gelderblom et al. 1988, da Rocha, Freire et al. 2014). The effect of fumonisins have been observed on cell morphology, cell-cell interactions, function of cell-surface proteins, protein kinases, lipid metabolism, cell growth, regeneration, and viability (Merrill Jr, Liotta et al. 1996).

2.1.3 Structure of FB₁

Fumonisin biochemical structure was first described in 1988, with prevalent isoforms, FB₁ and FB₂ (Bezuidenhout, Gelderblom et al. 1988) (Gelderblom, Jaskiewicz et al. 1988). FB₁ is a diester of propane 1,2,3-tricarballic acid and 2-amino-12, 16 dimethyl-3,5,10,14,15-pentahydroxycosane (Figure 2.3) (Bezuidenhout, Gelderblom et al. 1988).

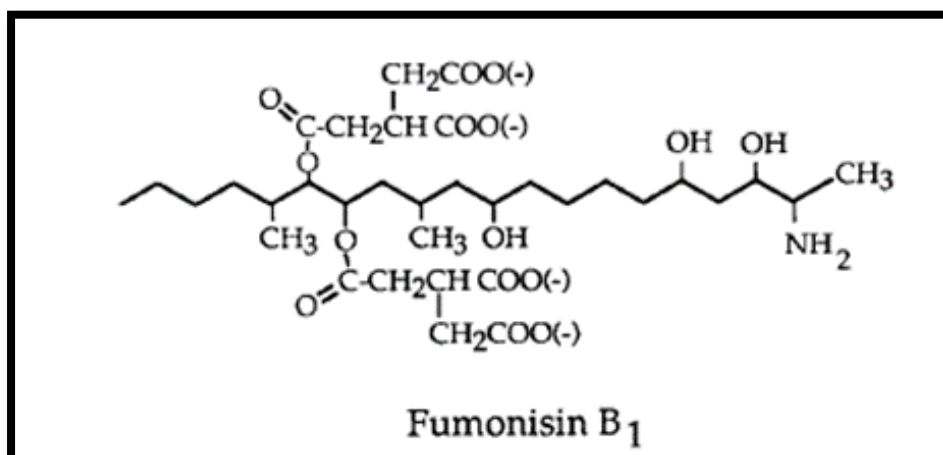


Figure 2.3: Structure of fumonisin B₁ (Merrill, Van Echten et al. 1993).

2.1.4 Mechanism of action

The structural resemblance of FB₁ to the sphingoid bases is critical to its ability to disrupt sphingolipid metabolism (Merrill Jr, Sullards et al. 2001, Riley, Enongene et al. 2001), this is due to the primary amine that is responsible for its biological activity (Norred, Riley et al. 2001, Fernandez-Surumay, Osweiler et al. 2005).

The similarity in structure between fumonisins and Sa and So allows FB₁ to inhibit ceramide synthase (Figure 2.4) (Soriano, Gonzalez et al. 2005). The Sa/So ratio maybe used as indicators of FB₁ exposure (Soriano, Gonzalez et al. 2005). Biological activity of FB₁ requires a free amino group, which makes FB₁ and other fumonisins with primary amino groups highly toxic compared to *N*-acetylated fumonisins, which leads to inhibition of ceramide biosynthesis, free So and Sa, and reduced reacylation of derived So from complex sphingolipids (Abbax, Gelderblom et al. 1993, Gelderblom, Cawood et al. 1993, Meeting 2001, Soriano, Gonzalez et al. 2005). All of these impact on cells health (Soriano, Gonzalez et al. 2005).

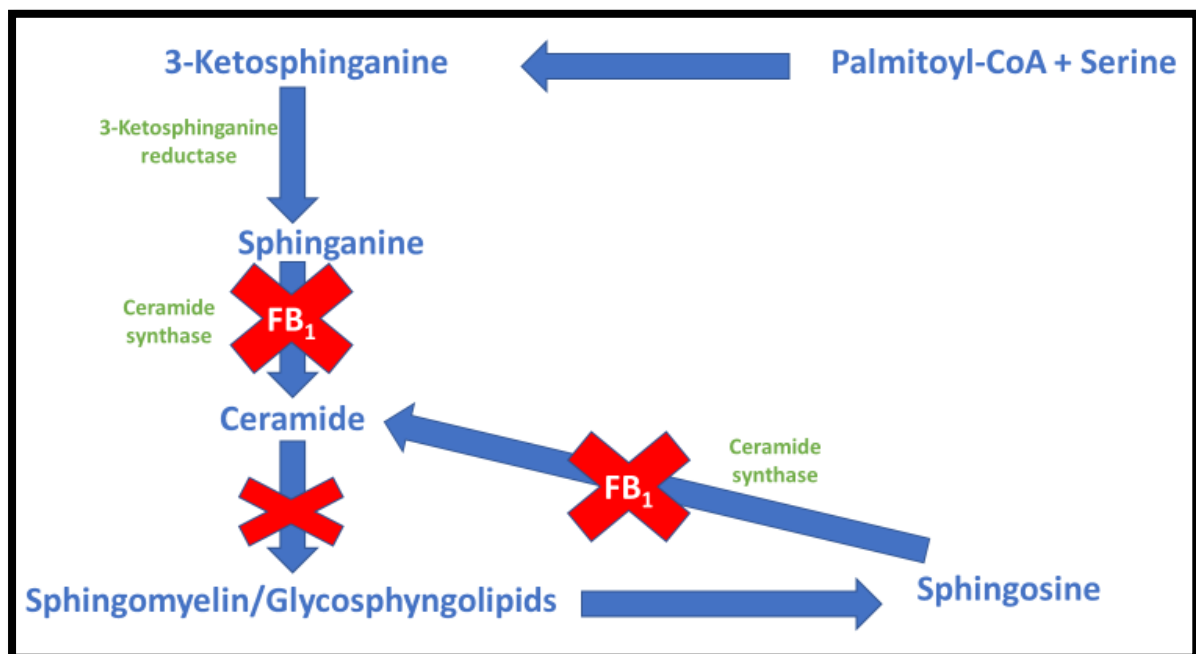


Figure 2.4: FB₁ disruption of sphingolipid metabolism (prepared by author).

2.1.4.1 Animals

Several studies have been conducted around the biochemical mechanisms of Fumonisin induced diseases in animals (Creppy 2002). Fumonisins are type dependent when affecting animals; ELEM is observed in horses and rabbits (Bucci, Hansen et al. 1996, Marasas, Kellerman et al. 2014), pulmonary oedema and hydrothorax in pigs (Harrison, Colvin et al. 1990), and it is hepatotoxic and carcinogenic in rats (Gelderblom, Kriek et al. 1991). FB₁ has also been shown to cause atherogenic effects in vervet monkeys (Fincham, Marasas et al. 1992), immunosuppression in poultry (Li, Ledoux et al. 1999) and brain haemorrhage in rabbits (Bucci, Hansen et al. 1996). Some studies have related FB₁ with the potential to be hepatotoxic to several animals (Harrison, Colvin et al. 1990).

2.1.4.2 Humans

The carcinogenic potential of FB₁ in humans has been well established. The natural occurrence of FB₁ in home-grown maize was associated with high rates of oesophageal cancer in Africa (Rheeder, Marasas et al. 1992, Thiel, Marasas et al. 1992), northern Italy (Franceschi, Bidoli et al. 1990), Iran (Shephard, Marasas et al. 2000) and the south east of the United States (Gelderblom, Marasas et al. 1992, Rheeder, Marasas et al. 1992). This toxin has also been linked with primary liver cancer in some regions of People's Republic of China (Chu and Li 1994, Groves, Zhang et al. 1999).

Fumonisin have also been linked with the outbreak of foodborne disease characterized by abdominal pain, borborygmic and diarrhoea in a several villages in India due to exposure to contaminated corn and sorghum intended for human consumption (Bhat, Shetty et al. 1997).

Neuronal tube defects (NTD) in offspring of pregnant woman consuming FB₁ contaminated maize is also a major adverse health outcome. This is a result of malformation of neuronal tubes in the brain and spinal cord (WHO. 2001). A major cause of NTD is folate deficiency, which alters sphingolipid content of cell membranes, compromising receptors such as the folate receptor and inhibits the uptake of folate, leading to complications such as NTD (Sadler, Merrill et al. 2002).

The data in the Chinese population indicate threatening levels of FB₁ and other mycotoxins in corn samples intended for human consumption, which are capable of producing carcinogenic nitrosamines that may play an important role in carcinogenesis in humans in Cixian and Linxian counties (Chu and Li 1994).

2.1.5 Molecular Toxicity

(A) Mitochondrial toxicity and oxidative stress

Fumonisin is non-genotoxic and non-DNA reactive, hence its carcinogenic effect indirectly affects DNA via cellular oxidative damage (Coulombe Jr 1993, Sahu, Eppley et al. 1998, Yin, Smith et al. 1998, Dragan, Bidlack et al. 2001). FB₁ inhibits mitochondrial complex I, decreases the rate of mitochondrial and cellular respiration, all of which leads to mitochondrial membrane depolarization and induction of ROS production (Domijan and Abramov 2011). FB₁ specifically targets the mitochondria, nucleus and nucleolus (Myburg, Needhi et al. 2009), and mitochondrial dysfunction has been suggested as a mechanism of FB₁ cytotoxicity (Domijan and Abramov 2011). Fumonisin accelerates the rate of oxidation, promotion of free radical intermediate production and chain reactions associated with lipid peroxidation (Yin, Smith et al. 1998). FB₁ induced lipid peroxidation might be an end result rather than a cause of FB₁-induced injury (Lemmer, Gelderblom et al. 1999).

(B) Cell Death and Apoptosis

A 2012 study revealed that FB₁ induced necrosis and apoptosis in the liver of rats (Gelderblom and Marasas 2012). FB₁ exerts neurotoxic effects by decreasing the activity of the glial cells (Kwon, Slikker Jr et al. 2000), inhibits axonal growth (Harel and Futerman 1993), impairs myelin formation and deposition and delays oligodendrocyte maturation (Monnet-Tschudi, Zurich et al. 1999). FB₁ has been shown to induce an increase of free sphinganine in HT29 cells, resulting in the significant reduction in cell number through growth inhibition and induction of apoptosis (Schmelz, Dombrink-Kurtzman et al. 1998).

(C) Epigenetic effects

Studies into the effect of FB₁ on the epigenetic landscape have been conflicted. It has been demonstrated that FB₁ induces a significant hypermethylation in DNA of C6 glioma cells at low concentrations (Mobio, Anane et al. 2000). FB₁ is associated with induction of global DNA hypomethylation and histone demethylation in HepG2 cells (Chuturgoon, Phulukdaree et al. 2014). FB₁ was also reported to down-regulate miR-27b in HepG2 cells, and inhibited apoptosis by upregulating the inhibitor of apoptosis family of proteins (Chuturgoon, Phulukdaree et al. 2014). These studies support the role of FB₁ being a hepatocarcinogen.

2.2 Neurotoxicity

Initiation of inflammation in the brain is triggered by the activation of microglial cells and astrocytes in response to injuries of the central nervous system (CNS), such as those caused by neurotoxic insults (Monnet-Tschudi, Zurich et al. 2007). Outcomes may be determined by the level of reactivity of glial and primary neuronal damage. Based on conditions, the brain inflammatory response can promote neuroprotection, regeneration or neurodegeneration, a mystery with regard to ELEM. It has been established that FB₁ is associated with NTD in human offspring exposed to FB₁ during gestation, which results in abnormal neuronal tubes in the brain and spinal cord (WHO. 2001). ROS is one of the potential causes of neuronal damage, as the brain is more sensitive to oxidative damage (Baek, Kwon et al. 1999).

2.3 Oxidative Stress

Overproduction of reactive oxygen species (ROS), such as superoxide radicals, hydrogen peroxide (H₂O₂), and hydroxyl radicals can have deleterious effects on cellular health (Wang, Wang et al. 2016). In the event that an imbalance of pro-oxidants outweighs antioxidants, then oxidative stress results (Jones 2006).

Experimental evidence supports the idea that compromised ROS homeostasis is involved in the development of numerous pathologies such as cardiovascular disease, neurodegenerative diseases, cancer and aging. The deleterious effects of free radicals depends on a number of factors, namely, the type of radical produced, the level, and the site of production, however, it is noteworthy that low concentrations of reactive species are essential to perform normal physiological functions like gene expression, cellular growth and defence against infection (López-Alarcón and Denicola 2013).

ROS have been linked with aging, cancer, autoimmune and neurodegenerative disorders, as a result of ROS disruptive abilities towards DNA through base damage, base removal, DNA strand breaks, protein-DNA cross linkage, mutations, deletions and translocations (Bayr 2005, Birben, Sahiner et al. 2012). ROS interacts with proteins, resulting in oxidation of amino acids (AA), especially sulphur-containing AA such as cysteine and methionine leading to changes to protein structure, unfolding and degradation (Birben, Sahiner et al. 2012). ROS also attacks lipids, leading to lipid peroxidation via oxidative degradation of lipids (Yin, Xu et al. 2011).

2.4 Antioxidant response

The transcription factor Nuclear-factor-erythroid 2 p45-Related Factor 2 (Nrf2) is a master regulator of the transcriptional response to oxidative stress (Solst, Rodman et al. 2017). Nrf2 is tightly linked with the coordination of the basal and inducible expression of antioxidant and Phase II detoxification enzymes that are essential for adaption to different stress conditions. Kelch-like ECH-associated protein 1 (Keap1) regulates the stability of Nrf2 and its cellular distribution. Nrf2 activities are also controlled by other numerous mechanisms such as posttranslational, transcriptional, translational and epigenetic, as well as by other protein partners (Nguyen, Sherratt et al. 2003, Nguyen, Nioi et al. 2009, Huang, Li et al. 2015). The classical pathway of Nrf2-regulated antioxidant response is via the Nrf2-Keap1 system as shown in Figure 2.5 (Ishii, Itoh et al. 2000).

In the inhibitory complex where Keap1 directly binds Nrf2 in the cytoplasm, Keap1 represses Nrf2 transactivation activity (Itoh, Wakabayashi et al. 1999). Under basal conditions, Keap1 ubiquitinates Nrf2 and localizes Nrf2 near the proteasome, thereby enhancing its degradation in the cytoplasm of quiescent cells. In instances of elevated cellular ROS however, the cysteine residues in the Nrf2/Keap1 complex oxidize, allowing Nrf2 to dissociate from Keap1 and translocate to the nucleus (Ishii, Itoh et al. 2000). In the nucleus, Nrf2 forms heterodimers with a group of nuclear bZIP proteins called small Maf proteins (Itoh, Igarashi et al. 1995). Nrf2 then induces expression of antioxidant genes via its interaction with regulatory DNA sequences in the antioxidant response element (ARE) (Solst, Rodman et al. 2017). The ARE or electrophile responsive element (EpRE) regulates the coordination in regulatory sites of target genes during the activation of antioxidants such as *GPx*, *SOD*, *HO-1*, *NQO1* (Friling, Bensimon et al. 1990, Rushmore, Morton et al. 1991, Eggler, Gay et al. 2008).

In order for Nrf2 to be activated it has to be phosphorylated (Huang, Nguyen et al. 2002). Protein Kinase C (PKC) catalyses the phosphorylation of Nrf2 at Ser40; this is a critical signalling event that results in cellular antioxidant response mediated by ARE (Huang, Nguyen et al. 2002). Ser40 is a critical residue of the domain in Nrf2-Keap1 interaction believed to be part of Neh2 (comprised of ≈ 100 N-terminal amino acids), which Keap1 binds through this domain of Nrf2 and PKC phosphorylates this domain at Ser40 upon oxidative stress, leading to a dissociation of Nrf2 from Keap1 (Huang, Nguyen et al. 2002).

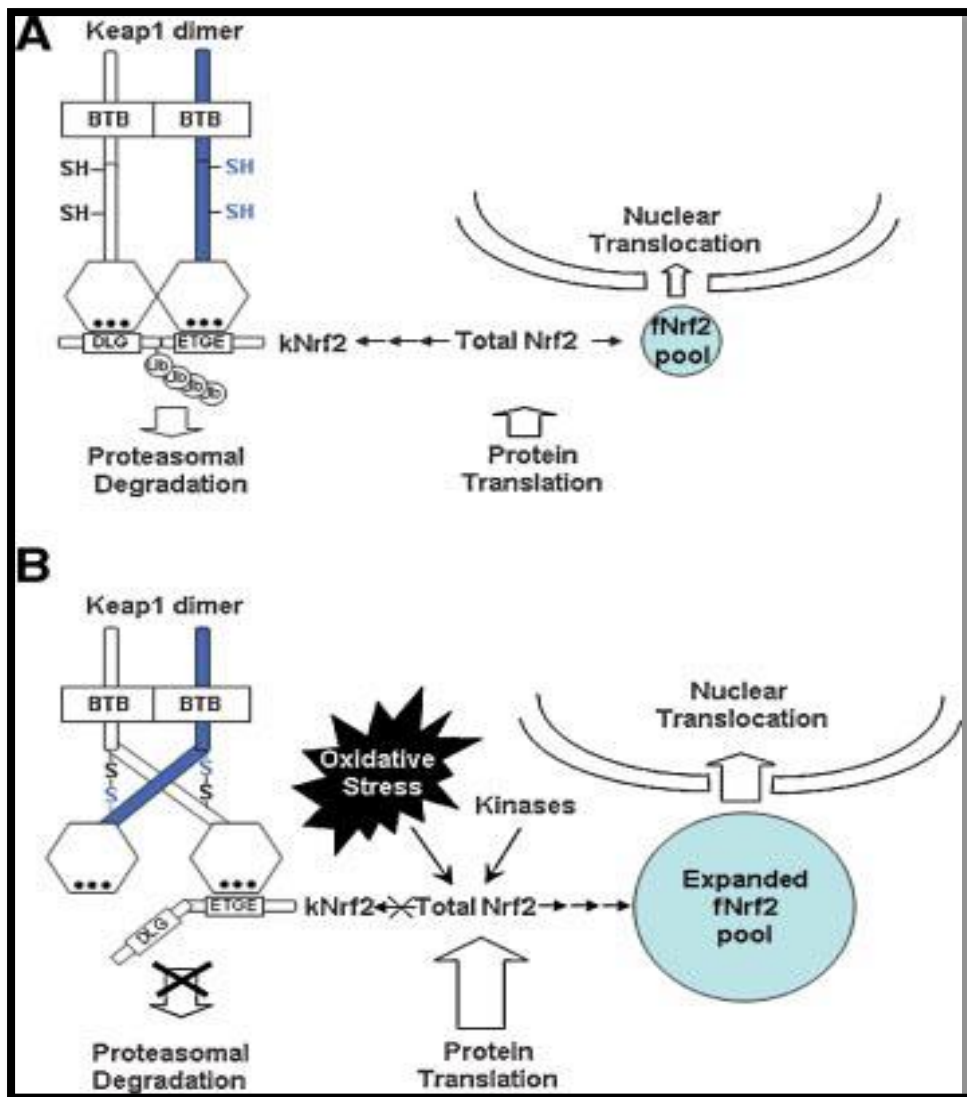


Figure 2.5: Proposed model of Nrf2-mediated redox signalling (Li and Kong 2009).

Detoxification of ROS is mediated by a network of antioxidant enzymes. Superoxide dismutase (SOD), Catalase (CAT), and Glutathione peroxidase (GPx) are the major antioxidant enzymes involved in radical scavenging. Superoxide dismutase acts as the first line of defence, catalysing the conversion of $O_2^{\cdot -}$ to H_2O_2 , while CAT and GPx further detoxify H_2O_2 to H_2O and O_2 respectively (Krinsky 1992).

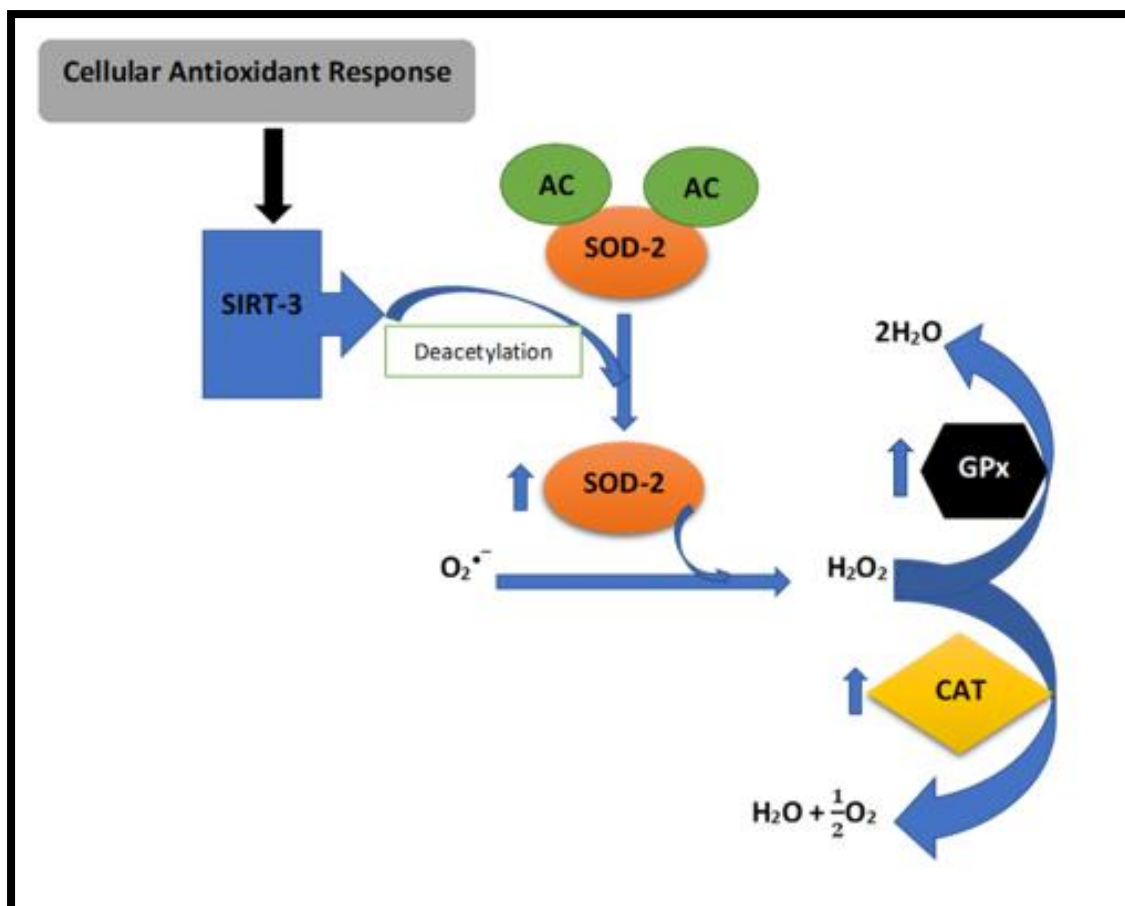


Figure 2.6: Radical scavenging activity of SOD, CAT, and GPx, starting from SIRT-3 (Prepared by author).

SOD-2, also known as manganese-dependent superoxide dismutase (MnSOD), is an enzyme which in humans is encoded by the *SOD2* gene located on chromosome 6 (Becuwe, Ennen et al. 2014). SOD2 functions to detoxify harmful superoxide radicals, produced during mitochondrial electron transport chain (ETC), into H_2O_2 and diatomic oxygen (Becuwe, Ennen et al. 2014) thereby, lowering ROS and conferring protection against cell death (Maslov, Naryzhnaia et al. 2015).

CAT is a common enzyme found in almost all living organisms, which are exposed to oxygen, where it functions to catalyse the conversion of hydrogen peroxide to H_2O and O_2 (Figure 6) (Lobo, Patil et al. 2010). CAT maintains the redox balance (Wang, Wang et al. 2016). Another antioxidant that detoxifies H_2O_2 is GPx, that uses low molecular weight thiols such as glutathione as cofactors. GPx contains the unique amino acid selenocysteine in its active sites and apart from converting H_2O_2 to H_2O , GPx also converts lipid peroxides to H_2O and its corresponding alcohols (Birben, Sahiner et al. 2012).

Mitochondrial maintenance

Sirtuin 3 (SIRT-3) is part of Sirtuin family, the mammalian homologues of the silent information regulator 3 (Liu, Chen et al. 2015). The encoded product of SIRT-3 is targeted to the mitochondrial cristae and SIRT-3 has an NAD⁺-dependent protein deacetylase activity (Onyango, Celic et al. 2002). SIRT-3 is a potential sensor NAD⁺/NADH ratios in the mitochondria. Elevated levels of NAD⁺ trigger a regulatory pathway that activate SIRT-3, leading to deacetylation of specific proteins (Onyango, Celic et al. 2002).

SIRT-3 reduces oxidative stress, maintains levels of bioenergetics, provides stability to the mitochondrial membranes, and improves neuronal Ca²⁺ handling (Cheng, Yang et al. 2016). SIRT-3 protects neurons against metabolic and oxidative stresses by activating SOD2, stabilizing cellular and mitochondrial Ca²⁺ homeostasis, and prevent apoptosis. It deacetylates and activates SOD-2, prevents excessive mitochondrial oxidative stress and its potential damage to cells (Cheng, Yang et al. 2016).

SOD-2 is a direct target of SIRT-3 (Qiu, Brown et al. 2010, Tao, Coleman et al. 2010, Tao, Vassilopoulos et al. 2014) and a major guardian of mitochondria in neurons. Some studies have suggested that SIRT-3 deacetylates and activates mitochondrial enzymes involved in fatty acid β -oxidation, amino acid metabolism, the electron transport chain, and antioxidant defences (He, Newman et al. 2012).

SIRT3 have multiple functions besides being a regulator of ROS scavenging, SIRT3 deacetylates Lon protease 1 (LONP1/ LON) to maintain mitochondrial structure and function (Gibellini, Pinti et al. 2014). LONP1 can be regulated by Nrf2 at a transcriptional level (Ngo, Pomatto et al. 2013). LONP1 functions to remove and degrades oxidatively damaged proteins in the mitochondria, which results in the prevention of cross linking and aggregation of damaged proteins, preventing mitochondrial dysfunction (Ngo and Davies 2009). Furthermore, LONP1 regulates mitochondrial gene expression and controls mtDNA copy number by degrading mitochondrial transcription factor A (Tfam) (Lu, Lee et al. 2013).

Mitochondrial transcription factor A (Tfam) is essential for mtDNA maintenance, and there is a directly proportional relationship between mitochondrial Tfam protein levels and mtDNA copy number (Rantanen, Jansson et al. 2001, Noack, Bednarek et al. 2006). The *in vitro* studies on Tfam, indicated that it is regulated through nuclear respiratory factors such as Nrf1 and Nrf2 in the nucleus. (Escrivá, Rodríguez-Peña et al. 1999, Matsushima, Goto et al. 2010).

There is a link between tau protein and oxidative stress, this link plays a huge role in the pathogenetic processes in neurodegenerations such as Alzheimer's disease (AD) (Cente, Filipcik et al. 2006). Previously it was shown that the human shortened form of the tau protein results in elevated levels of

reactive oxygen species, which leads to cell death in rat cortical neurons triggered by oxidative stress. This shows that shortened or compromised form of tau may trigger oxidative stress in the tauopathies and other neurodegenerative diseases such as AD (Cente, Filipcik et al. 2006).

2.5 miRNA

MicroRNAs (miRNAs) are 18 to 25 nucleotides long endogenous noncoding RNAs (Chen, Xu et al. 2014). The miRNAs function in regulation of gene expression at the posttranscriptional level by binding to complementary sites on target mRNAs leading to either an inhibition in mRNA translation or Breakdown of mRNA (Figure 2.7) (He and Hannon 2004, Chen, Xu et al. 2014). MicroRNAs have important functional roles in brain development and neuronal requirement but their function in neurodegenerative diseases such as AD is unclear (Cogswell, Ward et al. 2008).

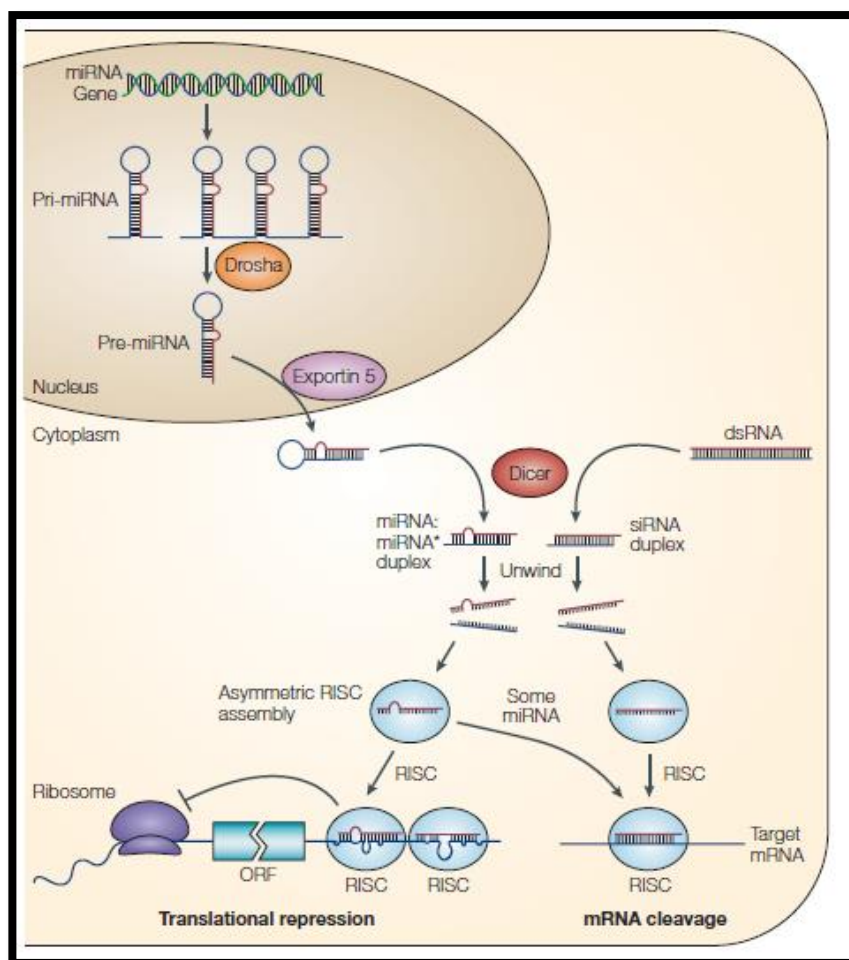


Figure 2.7: MiRNA biosynthesis and function (He and Hannon 2004). microRNA (miRNA); pri-microRNA (pri-miRNA); interfering RNA (siRNA)duplexes; RNA-induced silencing complex (RISC); open reading frame (ORF) (He and Hannon 2004).

The variety of miRNAs and the numerous genes that are targeted by a single miRNA provide endogenous noncoding RNAs with multipurpose functions in the control of gene expression (Chen, Xu et al. 2014). The *Keap1* 3'-UTR have one conserved miRNA targeting site, this was recognized by TargetScan5.1 prediction algorithm, this site is complementary to the miR-200 family members, miR-200a and miR-141 (which share identical seed sequences) (Eades, Yang et al. 2011). MiR-141 and miR-200a decrease Keap1 expression disrupting the Keap1-Nrf2 complex (Eades, Yang et al. 2011). Furthermore, the expression of miR-141 and miR-200a are induced by oxidative stress indicating a role of oxidative stress in the regulation of miR-141 and miR-200a.

2.6 Oxidative stress-induced diseases in the brain

Loss of ROS homeostasis has been reported in the pathogenesis of neurodegenerative diseases such as Alzheimer's disease (AD), dementia and cancer (Cente, Filipcik et al. 2006). Oxidative stress is elevated in the brain with AD and this may have a role in the pathogenesis of neuron degeneration and eventual death (Markesbery 1997). AD has been linked to mitochondrial defects affecting cytochrome-c oxidase, and these defects may contribute to the abnormal production of free radicals (Markesbery 1997). Understanding the mechanisms underlying the effects of abnormal levels of ROS in biological systems such as the brain can aid in therapeutic developments.

The role of oxidative stress, miRNAs and the activation of Nrf2 in pathogenesis of neurodegenerative diseases and cancer in the brain are currently of interest amongst researchers. FB₁ has been associated with cancer and neurodegenerative diseases but the underlying mechanisms by which this occurs is currently unclear. Therefore, the focus of this study was to investigate the effect of FB₁ on oxidative stress-related survival responses in male mice brain following 24 hours and 10 days exposure.

Chapter 3 - Materials and Methods

3.1 Materials

Fumonisin B₁ (FB₁) (F1147) was obtained from Sigma-Aldrich (St Louis, MO, USA). Western blot equipment and reagents were acquired from Bio-Rad (Hercules, CA, USA). Antibodies were purchased from Sigma-Aldrich (St Louis, MO, USA), Abcam (Cambridge, UK) and Cell Signalling Technology (Danvers, MA, USA). All other reagents were obtained from Merck (Darmstadt, Germany) unless otherwise stated.

3.2 Animal Treatment

This study was approved by the University of KwaZulu-Natal Animal Research Ethics Committee, Ethics Number: AREC/079/016. Animal treatments were conducted at Nelson Mandela Campus of University of KwaZulu-Natal AHRI building. Four groups of C57BL/6 black male mice (n= 5 per group) weighing approximately 20-22g: (1) Control groups (24 hrs and 10 days), (2) FB₁ 24 hrs exposed mice, and (3) FB₁ 10 days exposed mice. The control groups were exposed to 0.1M PBS upon acute (24 hrs) and prolonged (10 days) exposure. FB₁ was administered at 5mg/kg of FB₁ dissolved in 0.1M PBS at a rate of 0.25ml/23g orally in the experimental groups. Following 24 hrs and 10 days, control and FB₁ treated mice were sacrificed by halothane gassing. Brain tissue was harvested and rinsed in 0.1M PBS. Samples were then cut into approximately 1cm x 1cm pieces and stored in 500µl Qiazol and Cytobuster for RNA and protein isolation, respectively (Figure 3.1). All samples were stored at -80° C until further processing.

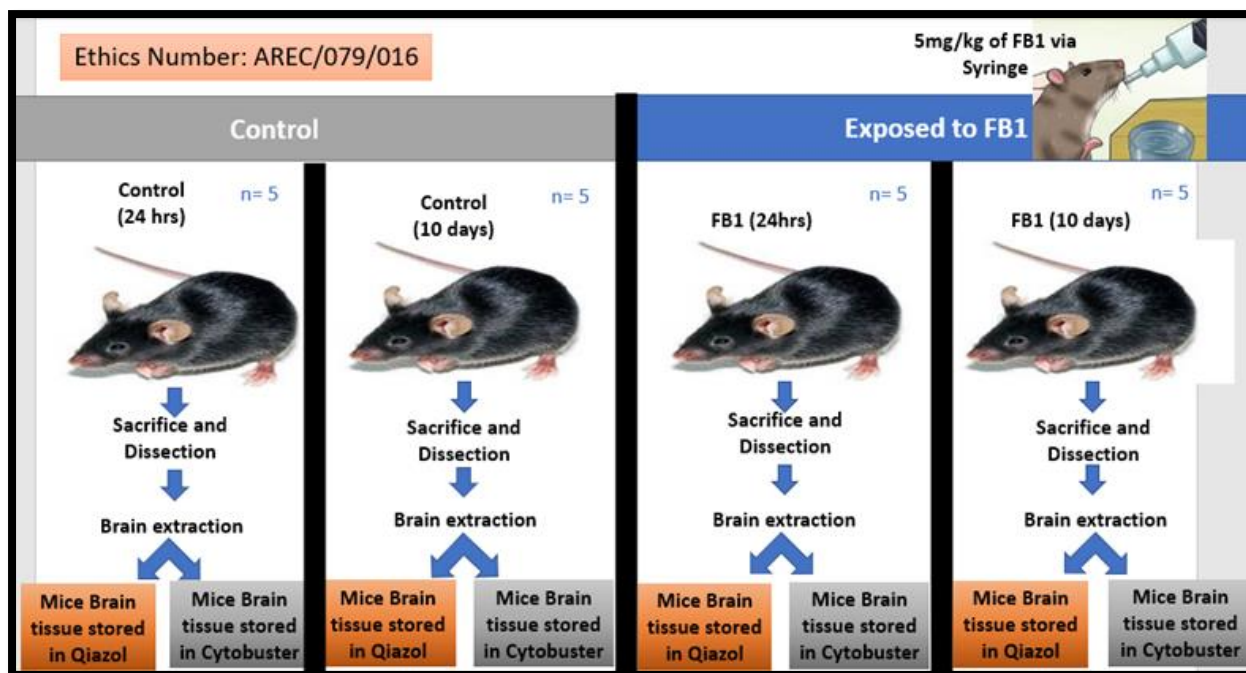


Figure 3.1: Animal treatment and brain extraction (Prepared by Author).

Sample Preparation - Homogenisation

Frozen samples in extraction buffers (Qiazol and Cytobuster) was done under the laminar flow hood. Samples were allowed to thaw on ice. Each sample was homogenised using a mechanical homogeniser until a slurry formed. Between each sample, the homogeniser was washed in detergent and 70% ethanol. Homogenates were transferred to 1.5ml microcentrifuge tubes and centrifuged (10 000 x g; 4°C; 10 min). The supernatants were aspirated and used for further extraction.

3.3 Protein expression – western blot

Introduction

Western blot is an analytical technique used to quantify the expression of a specific protein from a homogenous mixture of proteins extracted from cells and tissue. This procedure is based on the separation of proteins according to their size, transfer of these proteins to a solid support, detection of the proteins using immunoblotting and visualisation of protein bands using chemiluminescence (Eslami and Lujan 2010, Mahmood and Yang 2012).

3.4 Protein Isolation

Introduction

Using Cytobuster™ Protein Extraction Reagent (catalogue no. 71009, Novagen, Bloemfontein, SA), crude protein was isolated from mice brain tissue. Cytobuster is a non-ionic detergent that when combined with homogenisation allows for efficient extraction of soluble and functionally active proteins. To maintain protein integrity and prevent protein damage and degradation caused by the release of proteases and phosphatases during protein isolation, the Cytobuster lysis reagent is supplemented with a combination of protease and phosphatase inhibitors.

Protocol

The C57BL/6 mice brain tissues, stored in Cytobuster reagent (500µl) (Novagen, catalogue no. 71009) supplemented with a cocktail of protease inhibitors (Roche, catalogue no. 05892791001), were homogenised and centrifuged (10 000xg; 4°C; 10 min). Thereafter, the supernatant containing the crude protein was transferred to micro-centrifuge tubes and kept on ice.

3.5 Protein quantification and standardization

Principle

Bicinchoninic acid (BCA) assay was employed to determine protein concentration. This assay relies on two chemical reactions that occur under alkaline conditions. The first reaction is the biuret reaction, which involves the reduction of cupric ions (Cu^{2+}) to cuprous ions (Cu^{1+}) by peptide bonds (Figure 3.2). This is followed by the formation of a BCA- Cu^+ complex from Cu^+ ions and two molecules of BCA reacting together producing an intense purple colour that maximally absorbs light at a wavelength of 562nm. The amount of protein present in the sample can be measured by the intensity of the purple colour produced, since it is directly proportional to the number of peptide bonds participating in the reaction (Walker 1996, Huang, Long et al. 2010).

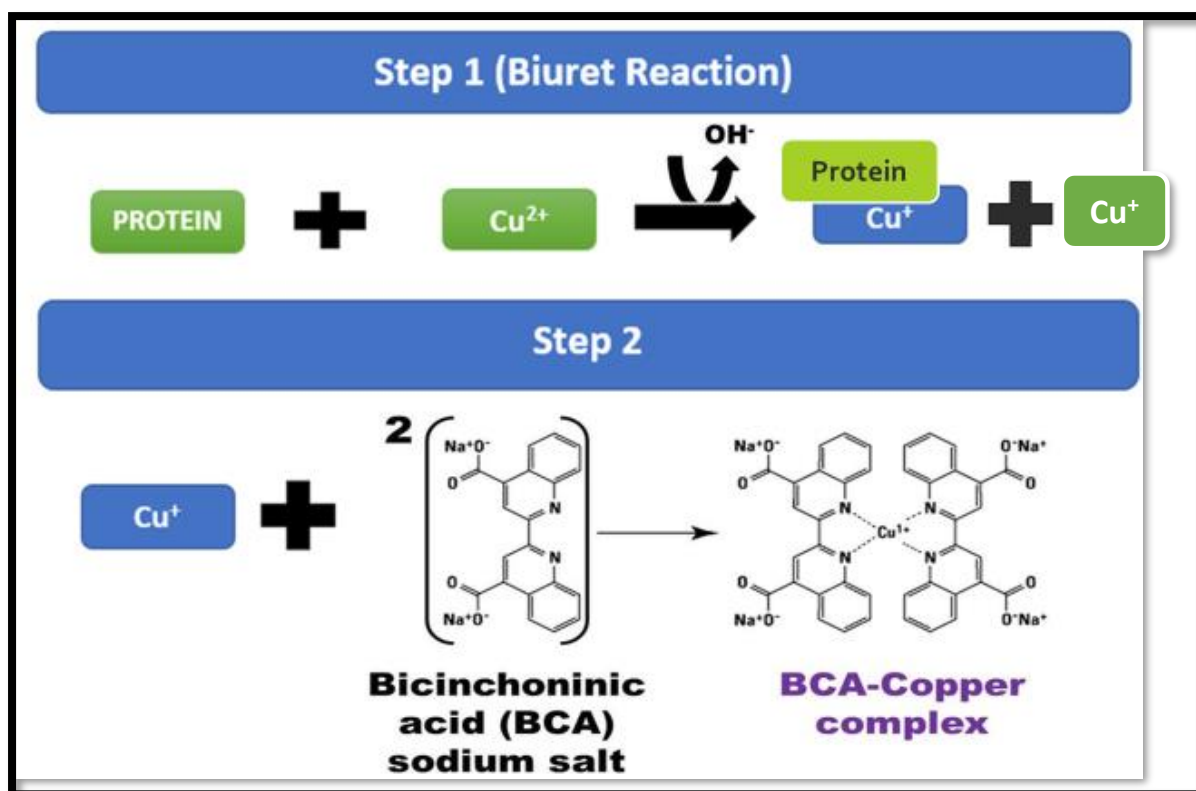


Figure 3.2: Presentation of the BCA assay principle (prepared by author).

Protocol

Bovine serum albumin (BSA) standards [0, 0.2, 0.4, 0.6, 0.8 and 1mg/ml] were dissolved in distilled water. The standard curve was constructed using the absorbances of the BSA standards, which allowed the concentration of protein present in each sample to be determined. Following standard preparation, plating was conducted by pipetting 25µl of each standard (triplicate) and protein sample (duplicate) into a 96-well microtiter plate. A combination of 198µl BCA and 4µl CuSO₄, forming a working solution (200µl) was added to each well and the plate was incubated at 37°C for 30 min. Thereafter, the absorbance was measured at 562nm using a spectrophotometer (Bio-tek µQuant Plate Reader).

Proteins were standardised to a concentration of 1mg/ml in Cytobuster reagent and boiled (100°C) in Laemmli buffer [dH₂O, 0.5M Tris-HCl (pH 6.8), glycerol, 10% SDS, 5% β-mercaptoethanol and 1% bromophenol blue] for 5 min. In Laemmli buffer, Tris-HCl maintains pH, glycerol adds weight to the samples allowing the samples to sink into the wells of the gel (Mahmood and Yang 2012), and bromophenol blue enables the samples to be visualised as they migrate through the gel in SDS-PAGE. SDS allows the proteins to be separated based on their molecular weights by denaturing and imparting an overall negative charge to the proteins (Mahmood and Yang 2012). The β-mercaptoethanol breaks disulphide bonds further denaturing proteins. All protein samples were allowed to adjust to RT prior to storing at -20°C.

3.6 Sodium dodecyl sulphate–polyacrylamide gel electrophoresis (SDS-PAGE) and Western Blotting

Preparation of Gels for SDS-PAGE

Introduction

Polyacrylamide gels are a 3D polymer consisting of acrylamide and a cross-linker known as N, N'-methylene bis-acrylamide catalysed by ammonium persulfate (APS). SDS-PAGE employs two types of agarose gels to separate proteins according to their molecular weights. The upper gel, known as the stacking gel, is slightly acidic (pH 6.8) and contains large pores that poorly separate proteins due to its low polyacrylamide content (Mahmood and Yang 2012), however, the stacking gel allows the proteins to form thin sharply defined bands for separation by the lower resolving gel. The resolving gel is basic (pH 8.8), has a high polyacrylamide content and narrow pores that enable the proteins to be separated according to their molecular weights (Mahmood and Yang 2012).

Protocol

The Mini-PROTEAN Tetra Cell casting stand (BioRad) was used to prepare gels for SDS-PAGE (Figure 3.4). The 10% resolving gel [dH₂O, 1.5M Tris (pH 8.8), 10% SDS, bis-acrylamide, 10% APS and TEMED] was prepared first and allowed to polymerize for 1 hr, followed by the preparation and addition of the 4% stacking gel [dH₂O, 0.5M Tris (pH 6.8), 10% SDS, bis-acrylamide, 10% APS and TEMED]. A 1.5mm plastic comb was placed between the glass plates to enable the formation of wells for sample loading (Figure 3.3) and the gel was allowed to set for approximately 45 min.

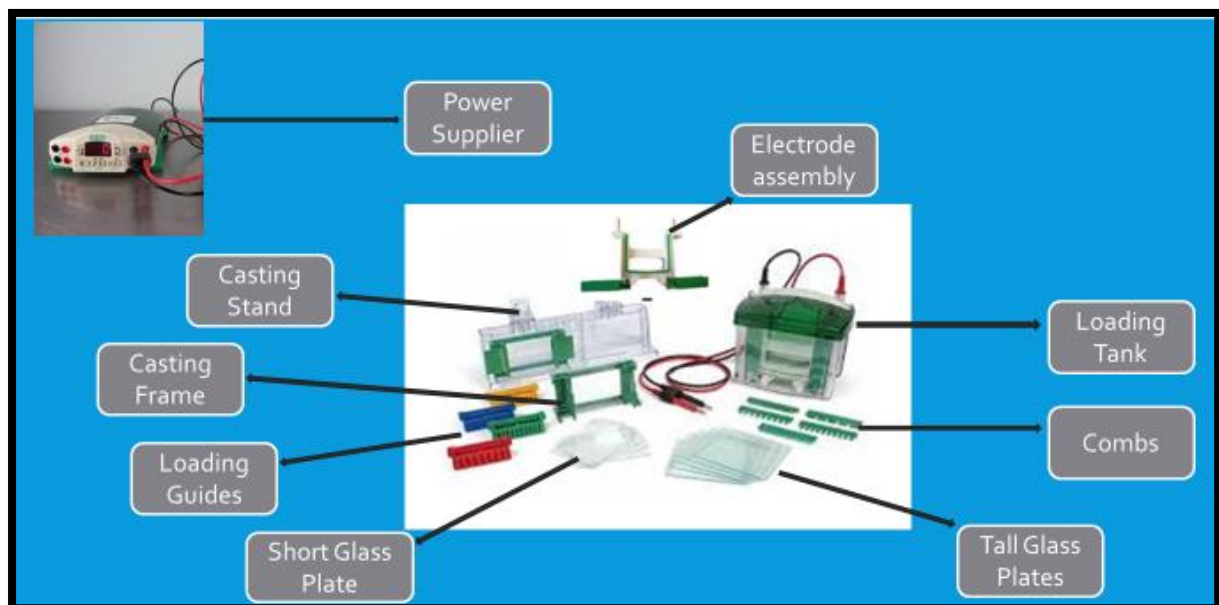


Figure 3.3: Equipment used to prepare SDS-PAGE gels (Prepared by author)

SDS-PAGE

The gel cassettes were placed into the electrode tank (Mini-PROTEAN Tetra Cell System, Bio-Rad) and the tank was filled 1X running buffer [25mM Tris, 192mM glycine and 0.1% SDS]. The molecular weight marker (5µl) (Precision Plus Protein All Blue Standards, catalogue no. #161-0373, Bio-Rad) and protein samples (25µl) were then loaded into the wells and the samples were electrophoresed (150V, 1.5 hrs) using the Bio-Rad compact power supply.

Protein Transfer

Following electrophoresis, proteins that were separated are transferred to a nitrocellulose membrane. The gels were removed from the glass plates and the stacking gel was detached leaving only the resolving gel. The gel together with the nitrocellulose membrane and two fibre pads were equilibrated in transfer buffer [25mM Tris, 192mM glycine and 20% methanol, pH 8.3] for 10 min. Following equilibration, a sandwich of a fibre pad, nitrocellulose membrane, gel and fibre pad was placed in the transfer cassette and the separated proteins were electro-transferred to the nitrocellulose membrane using the Trans-Blot Turbo Transfer System (30 min, 25V; Bio-Rad). The negatively charged proteins migrate out of the gel onto the nitrocellulose membrane due to the voltage generating an electric current perpendicular to the surface of the gel.

Blocking and Antibody Incubation

Following transfer, the non-specific binding of proteins was prevented by incubating (1hrs, RT) the membranes in 5% BSA in Tris buffered saline with 0.05% Tween 20 [TTBS; 150mM NaCl, 3mM KCl, 25mM Tris, 0.05% Tween 20, dH₂O, pH 7.5]. Thereafter, the primary antibody (Table 1) of interest was added to the membranes for 1 hr on the shaker at RT and then overnight at 4°C. Following the overnight incubation, the membranes were equilibrated to RT and washed five times with TTBS (10 min each, RT) to remove unbound primary antibody. The membranes were then probed with the respective horse-radish peroxidase (HRP)-conjugated secondary antibody (Table 3.1) for 2 hrs at RT with gentle shaking. The specificity of the secondary antibody will allow it to bind only to the primary antibody of interest. Following incubation, unbound secondary antibody were removed by washing the membranes five times with TTBS (10 min each, RT).

Table 3.1: Antibodies, antibody dilutions and catalogue numbers.

	ANTIBODY	DILUTION	CATALOGUE NUMBER
Primary Antibodies	Rabbit Anti-pNrf2 (phosphorylated-serine 40)	1:1 000 in 5% BSA	Ab76026 (Abcam)
	Rabbit Anti-Nrf2	1:1 000 in 5% BSA	12721S (Cell signalling technology)
	Mouse Anti-CAT	1:1 000 in 5% BSA	C0979 (Sigma- Aldrich)
Secondary Antibodies	Goat Anti-mouse IgG HRP	1:10 000	7074S (Cell signalling technology)
	Goat Anti-rabbit IgG HRP	1:10 000	7076P2 (Cell signalling technology)
Housekeeping antibody	Anti- β -actin	1:5 000 in 5% BSA	A3854 (Sigma-Aldrich)

Imaging

The antigen-antibody complex was visualised using the Clarity™ Western ECL Substrate Kit (catalogue no. #170-5060, Bio-Rad) and the ChemiDoc™ XRS+ Molecular Imaging System (Bio-Rad). The Clarity™ western ECL Substrate kit consisting of a hydrogen peroxide substrate and an enhanced luminol solution. The HRP conjugated to the secondary antibody reacts with the H₂O₂ substrate to yield oxygen radicals which react and degrade the luminol into aminophthalic acid. The aminophthalic acid then reacts with enhancer molecules causing it to luminesce enabling the visualization of protein bands (Figure 3.4).

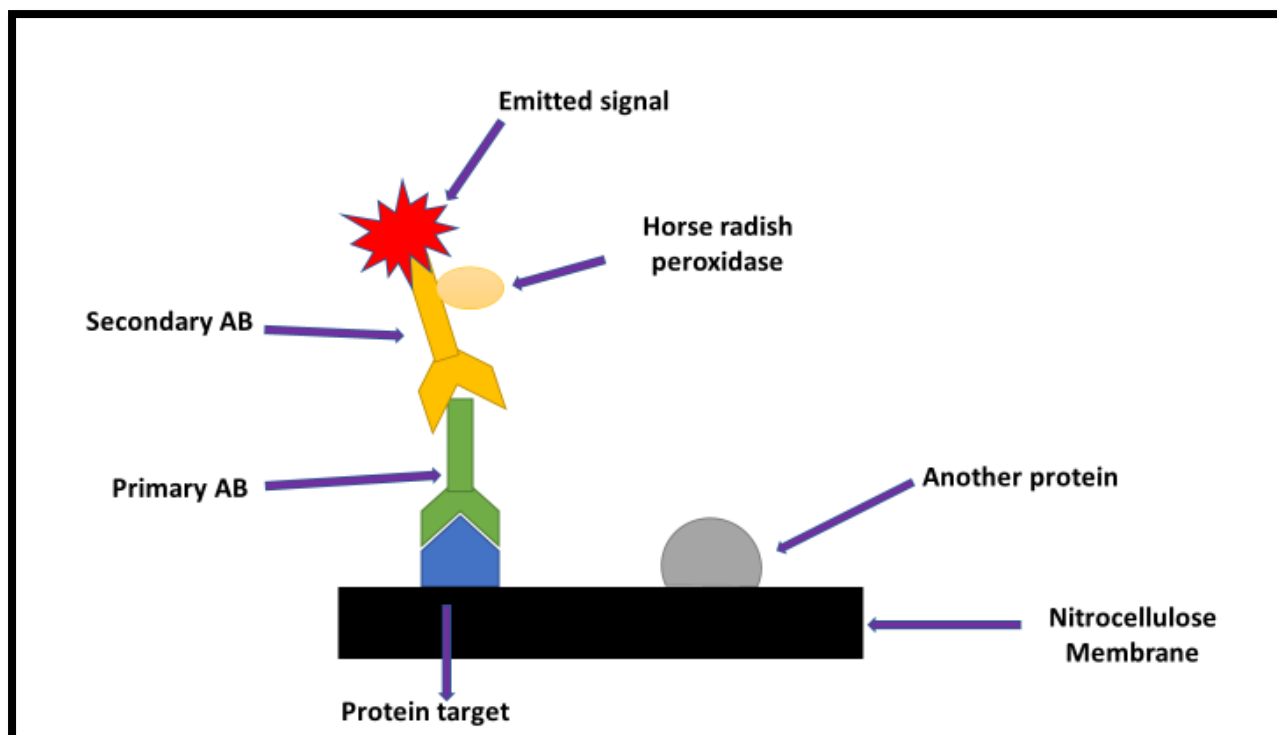


Figure 3.4: Immunoblotting and protein detection (Prepared by author)

Quenching and Normalisation

Following detection, H_2O_2 (5ml) (30 min, 37°C) was used to quench the membranes. Thereafter, the membranes were washed once with TTBS (10 min, RT), blocked in 5% BSA in TTBS (1 hr, RT) and probed (30 min, RT) with the housekeeping protein, anti- β -actin (Table 1) to normalise protein expression.

Image Lab Software version 5.0 (Bio-Rad) was employed to analyse protein expression and the results were expressed as percentage (%) fold-change and band density.

3.7 Gene expression – Quantitative polymerase chain reaction

Principle

Quantitative polymerase chain reaction (qPCR) is a simple tool used to rapidly amplify specific gene sequences *in vitro* from a template strand. Two complementary oligonucleotide primers to the sites flanking the target region are synthesised chemically. *Taq* polymerase which is thermostable, synthesises complementary DNA (cDNA) strands by adding deoxynucleotide triphosphates (dNTPs) to oligonucleoside primers that are complementary to the DNA sequence flanking the target gene (Pestana,

Belak et al. 2010). The thermocycler is used to perform PCR where it undergoes repetitive cycling of three incubation steps at different temperatures (Figure 3.5). The three steps include:

1. Denaturation: At 95°C Double stranded (ds) DNA is denatured to form single stranded (ss) DNA.
2. Annealing: At 55°C Complementary primers to the target sequence are annealed to the template DNA.
3. Extension: At 72°C, annealed primers are extended by a DNA polymerase (Taq DNA polymerase). Each cycle amplifies the target copy. This results in exponential amplification of the original DNA fragment.

These three steps make up one cycle of a PCR reaction (Figure 3.6). This cycle is repeated 30 to 40 times to achieve sufficient amplification (Arya, Shergill et al. 2005).

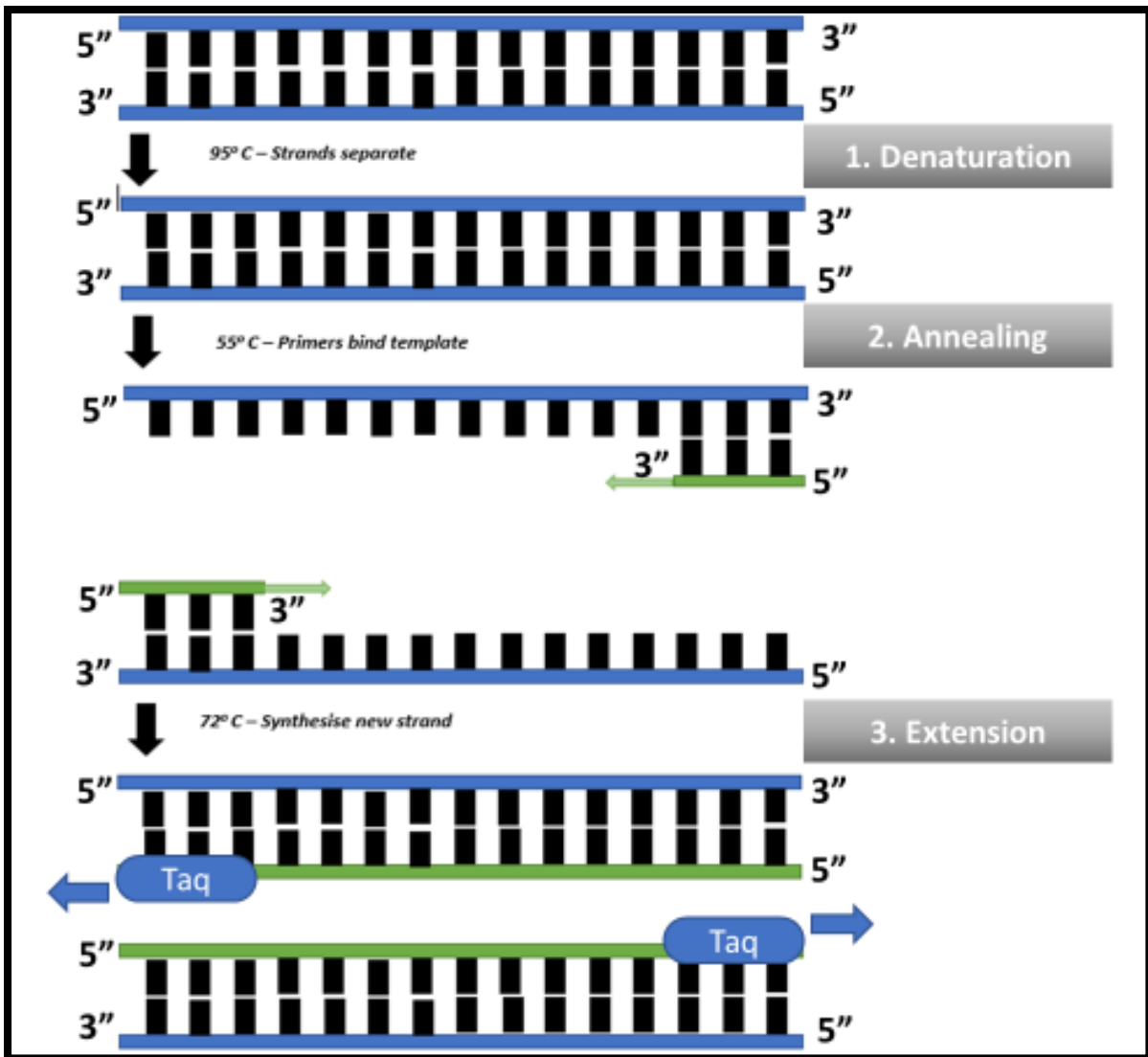


Figure 3.5: Presentation of a single PCR cycle, during DNA amplification (Prepared by author).

PCR requires the following to occur:

- DNA template – contains the sequence of interest
- Forward and Reverse primers – Binds to the 3' ends of the forward and reverse strands of the target sequence
- *Taq* polymerase – Catalyses the synthesis of new strands of DNA complementary to the sequence of interest, by adding nucleotides to the ends of the annealed primers
- Deoxynucleoside triphosphates (dNTPs) –Required Building blocks for the synthesis of new DNA strands
- $MgCl_2$ – Stabilizes DNA and ensures the optimal functioning of *Taq* polymerase. It acts as a cofactor for *Taq* polymerase
- Buffer system – Maintains optimum pH for PCR reaction to occur

Quantitative PCR (qPCR) can quantify PCR amplicons, unlike conventional PCR which allows for the exponential amplification of the DNA target sequence, without the ability to quantify PCR amplicons. Quantitative PCR can measure the PCR amplicons generated during each cycle of the PCR process (Pestana, Belak et al. 2010). Amplicons are detected using the DNA-intercalating dye, SYBR® Green 1 (Figure 3.6), which fluoresces intensely when it binds to the minor groves of double stranded DNA. The double stranded DNA present is directly proportional to the intensity of the florescence (Arya, Shergill et al. 2005).

Simultaneously with the gene of interest, samples are analysed for expression of a house keeping gene, and the amount of target DNA is reported relative to the amount of the house keeping gene for each sample. Analysis of gene expression is conducted by comparing the target gene with the house-keeping gene using the Livak and Schmittgen ($2^{-\Delta\Delta CT}$) method and reported as fold change (Livak and Schmittgen 2001).

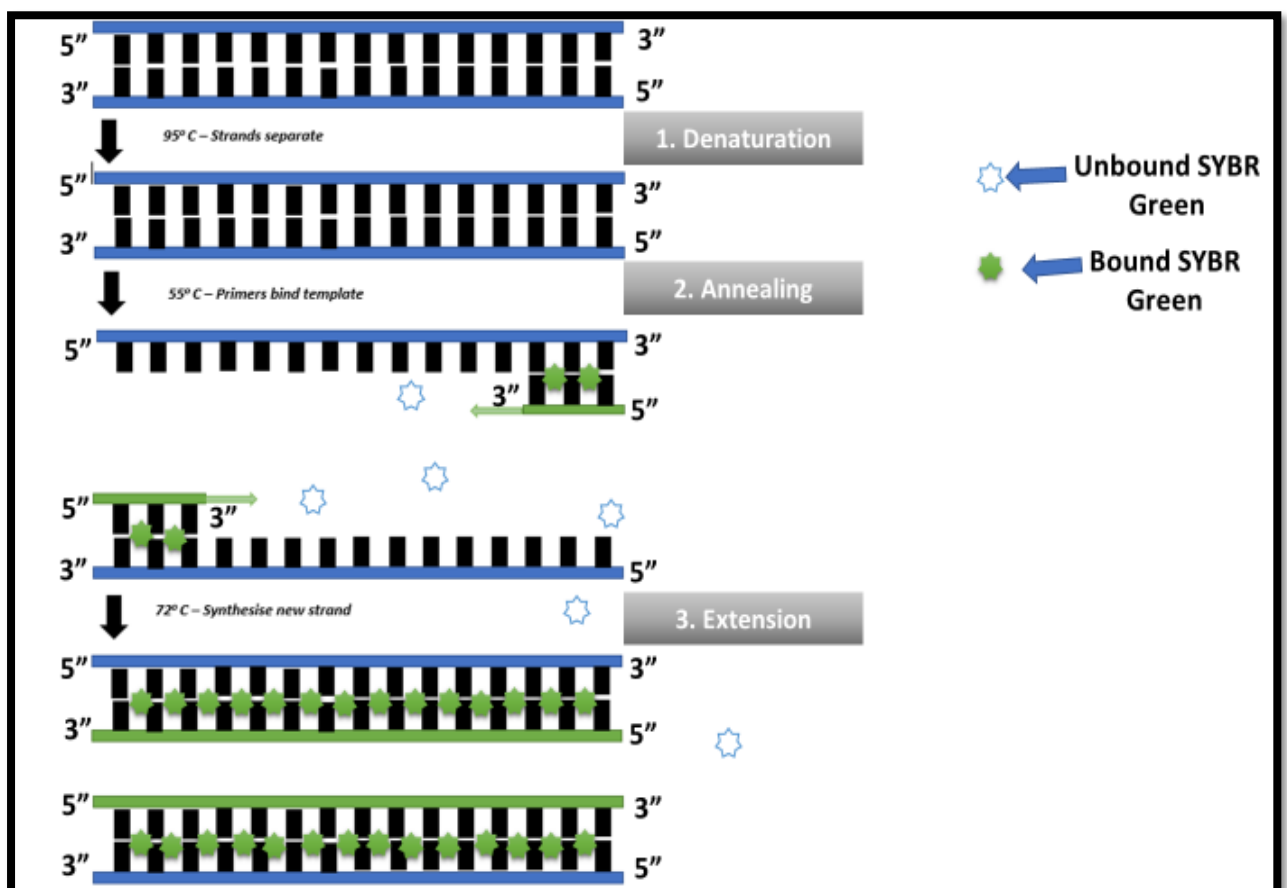


Figure 3.6: Fluorescence increases drastically when dye molecules bind to dsDNA (Prepared by author)

Protocol

RNA was isolated from control, FB₁ (24 hrs) and FB₁ (10 days) homogenates in 500µl Qiazol after being incubated at -80°C overnight. The samples were thawed at RT, chloroform (100µl) was then added and centrifuged (12,000Xg, 15 min, 4°C). The aqueous layer containing the crude RNA was transferred into fresh 1.5ml micro-centrifuge tubes and isopropanol (250 µl, 1 h, -80°C) was added. The samples were centrifuged (12,000Xg, 20 min, 4°C), RNA pellets were then washed with 75% ethanol (500µl) and centrifuged (7,400Xg, 15 min, 4°C). Following removal of ethanol, RNA pellets were air dried for approximately 2 hrs and re-suspended in 15µl of nuclease-free water. The RNA was quantified using the Nanodrop2000 spectrophotometer (Thermo-Fisher Scientific) and standardised to 1,000 ng/µl. A 20 µl reaction volume containing 1 µl RNA template, 4 µl 5X iScript™ reaction mix, 1 µl iScript reverse transcriptase and nuclease free water was used to synthesize cDNA (iScript™ cDNA Synthesis kit, Bio-Rad; catalogue no 107-8890). Thermocycler conditions were 25°C for 5 min, 42°C for 30 min, 85°C for 5 min and a final hold at 4°C.

Analysis of gene expression was conducted by employing the SsoAdvanced™ Universal SYBR® Green Supermix (catalogue no. #172-5271, Bio-Rad), according to manufacturer's instructions. The mRNA expressions of *SOD-2*, *Tfam*, *GPx*, *Nrf-2*, *Tau*, *SIRT-3*, *LONP1* were investigated using specific forward and reverse primers (Table 2). *GAPDH* was used as a house-keeping gene. Reaction volumes consisting of the following were prepared: SYBR green (5µl), forward primer (1µl), reverse primer (1µl), nuclease free water (2µl) and cDNA template (1000ng/µl, 1µl). All reactions were carried out in triplicate.

The amplification of samples was done using a CFX96 Touch™ Real-Time PCR Detection System (Bio-Rad). The initial denaturation occurred at 95°C (8 min), followed by 40 cycles of denaturation [95°C, 15 second (sec)]; annealing (40sec; Temperatures – Table 3.2) and extension (72°C, 30 sec) followed by a plate read. The method described by Livak and Schmittgen was employed to determine the relative changes in mRNA expression, where $2^{-\Delta\Delta CT}$ represents the fold change observed in mRNA expression (Livak and Schmittgen 2001). The expression of the gene of interest was normalised against the house-keeping gene, *GAPDH*, which was amplified simultaneously under the same conditions.

Table 3.2: The gene of interest, annealing temperatures and primer sequences.

Gene	Annealing temperature	Primer	Sequence
<i>SOD-2</i>	61.4°C	Forward	5'-CAGACCTGCCTTACGACTATGG-3'
		Reverse	5'-CTCGGTGGCGTTGAGATTGTT-3'
<i>Tfam</i>	61°C	Forward	5'-TGAAGCTTGTAATGAGGCTTGGA-3'
		Reverse	5'-CGGATCGTTTCACACTTCGAC-3'
<i>GPx</i>	61.4°C	Forward	5'-GGGACTACACCGAGATGAACGA-3'
		Reverse	5'-ACCATTCACTTCGCACTTCTCA-3'
<i>Nrf-2</i>	58°C	Forward	5'-CTTTAGTCAGCGACAGAAGGAC-3'
		Reverse	5'-AGGCATCTTGTTTGGGAATGTG-3'
<i>Tau</i>	61°C	Forward	5'-TGGGGAACATTCCGTATGAGG-3'
		Reverse	5'-CAGAAGCCATAACCCTTGGG-3'
<i>SIRT3</i>	60°C	Forward	5'-GAGCGGCCTCTACAGCAAC-3'
		Reverse	5'-GGAAGTAGTGAGTGACATTGGG-3'
<i>LONP1</i>	60°C	Forward	5'-CTCATGGTGGAGGTTGAGAATG-3'
		Reverse	5'-CAGAGGGTTCAAGGCGATGAT-3'
<i>GAPDH</i>	Housekeeping	Forward	5'-ATGTGTCCGTCGTGGATCTGAC-3'
		Reverse	5'-AGACAACCTGGTCCTCAGTGTAG-3'

MicroRNA Assay

The total RNA extracted (as previously described) was reverse transcribed using the miScript® II RT Kit (Qiagen, Hilden, Germany; catalogue number 218160) as per manufacturer's instructions. To quantify miRNA levels, *miR-141* (MS00001610) miScript Primer Assays was used, while *RNU6* (MS00033740) was used as an internal control (Qiagen, Hilden, Germany). Experimental protocol was performed as per manufacturer's instructions. The reaction was carried out with an initial activation step (95°C, 15 min), followed by 40 cycles of denaturation (94°C, 15 sec), annealing (55°C, 30 sec), extension (70°C, 30 sec) and a plate read. Assays were conducted using CFX Touch™ Real Time PCR Detection System (Bio-Rad). The analysis of data was conducted using the method described by Livak and Schmittgen ($2^{-\Delta\Delta CT}$) (Livak and Schmittgen 2001).

3.8 Statistical Analyses

Microsoft Excel 2016 and GraphPad Prism version 5.0 (GraphPad Software Inc., California) were employed to perform all statistical analyses. The unpaired t-test with Welch's Correction was used for all assays. All results were represented as the mean \pm standard deviation unless otherwise stated. A value of $p < 0.05$ was considered statistically significant.

Chapter 4 – Results

4.1 Western Blot

4.1.1 Antioxidant response

FB₁ triggered a response of AO proteins in C57BL/6 mice brain as result of increased ROS production. The key regulator of endogenous AO is Nrf2. In Figure 4.1, the protein expression of total Nrf2 and pNrf2, were significantly increased after 24hrs exposure and decreased after 10 day exposure to FB₁ (total Nrf2; 24hrs: * $p=0,0144$ (Control: 0.5820 ± 0.1453 RBD vs. FB₁: 0.8160 ± 0.1174 RBD); 10 days: ** $p=0,0094$ (Control: 0.5780 ± 0.08817 RBD vs. FB₁: 0.5380 ± 0.1640 RBD)) (phosphorylated Nrf2; 24hrs: * $p=0,0132$ (Control: 0.9203 ± 0.3320 RBD vs. FB₁: 0.6603 ± 0.1917 RBD); 10 days: * $p=0,0462$ (Control: 1.150 ± 0.5470 RBD vs FB₁: 1.278 ± 0.5192 RBD)).

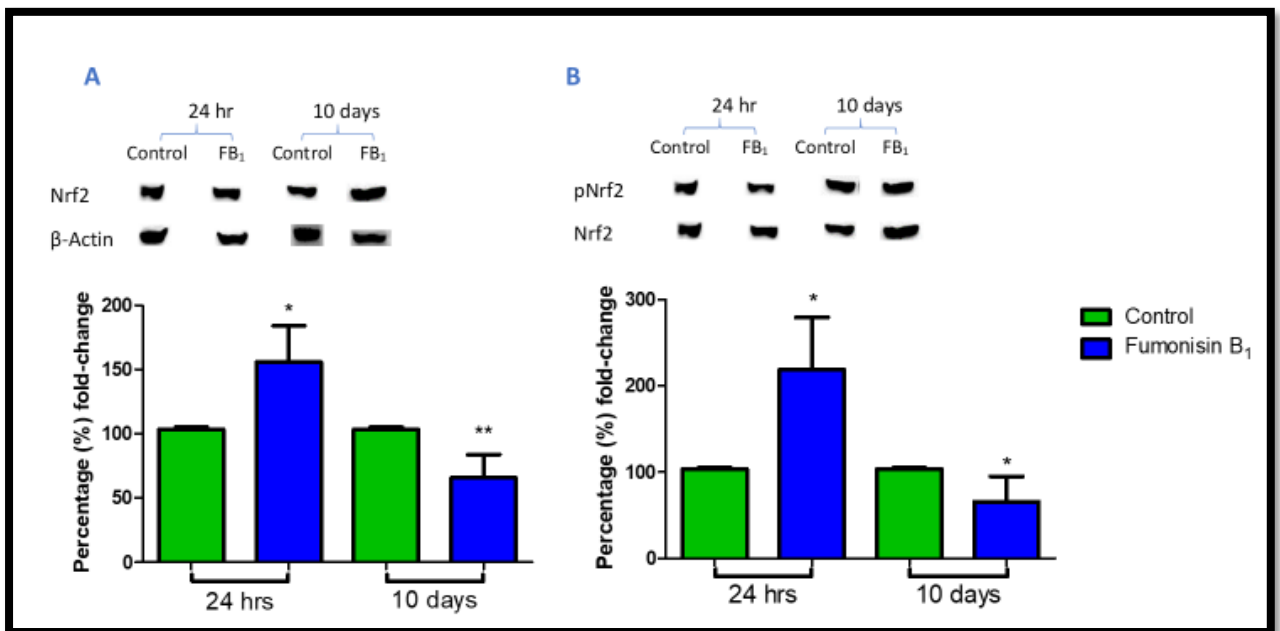


Figure 4.1: (A) Protein expression of Nrf2 (24hrs: * $p=0,0144$; 10 days: ** $p=0,0094$), (B) Protein expression of pNrf2 (24hrs: * $p=0,0132$; 10 days: * $p=0,0462$) in mice brain exposed to FB₁.

4.1.2 Detoxification of peroxides

Catalase (CAT), a common enzyme found in nearly all living organisms, is upregulated during oxidative stress and functions to catalyse the decomposition of hydrogen peroxide to water and oxygen. FB₁ non-significantly increased the protein expression of CAT in mice brain following acute (24 hrs: Control: 1.628 ± 0.4824 RBD vs. FB₁: 1.426 ± 0.4842 RBD, $p= 0,1206$; Figure 4.2) and significantly increased expression upon prolonged exposure (10 days: Control: 0.9860 ± 0.03027 RBD vs. FB₁: 1.056 ± 0.1428 RBD, $**p= 0,0010$; Figure 4.2).

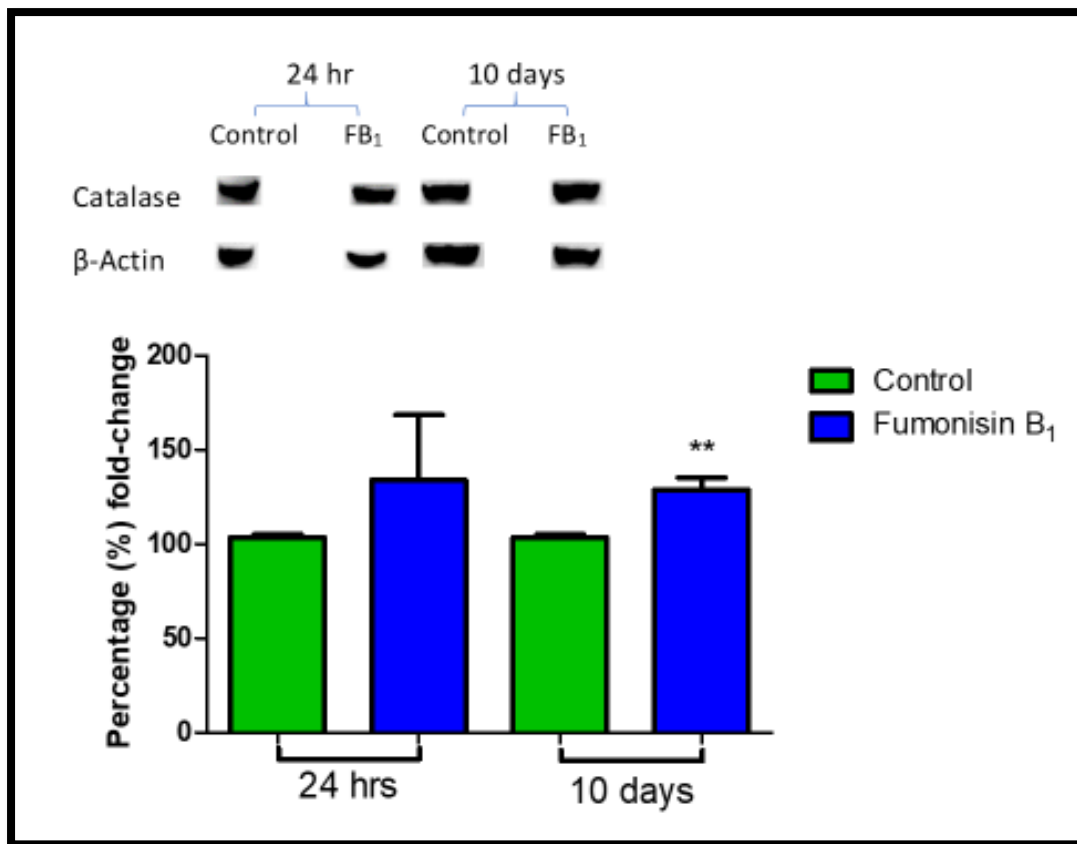


Figure 4.2: Protein expression of Catalase in mice brain exposed to FB₁ for 24hrs ($p= 0,1206$) and 10 days ($**p= 0,0010$).

4.2 Quantitative polymerase chain reaction (qPCR)

4.2.1 Antioxidant response

To validate the expression of Nrf2 observed at the protein level, *Nrf2* mRNA expression was investigated using qPCR. FB₁ significantly decreased the mRNA expression of *Nrf2* in mice brain following acute (24hrs: *** $p=0,0001$; Figure 4.3) and prolonged (10 days: ** $p=0,0013$; Figure 4.3) exposure.

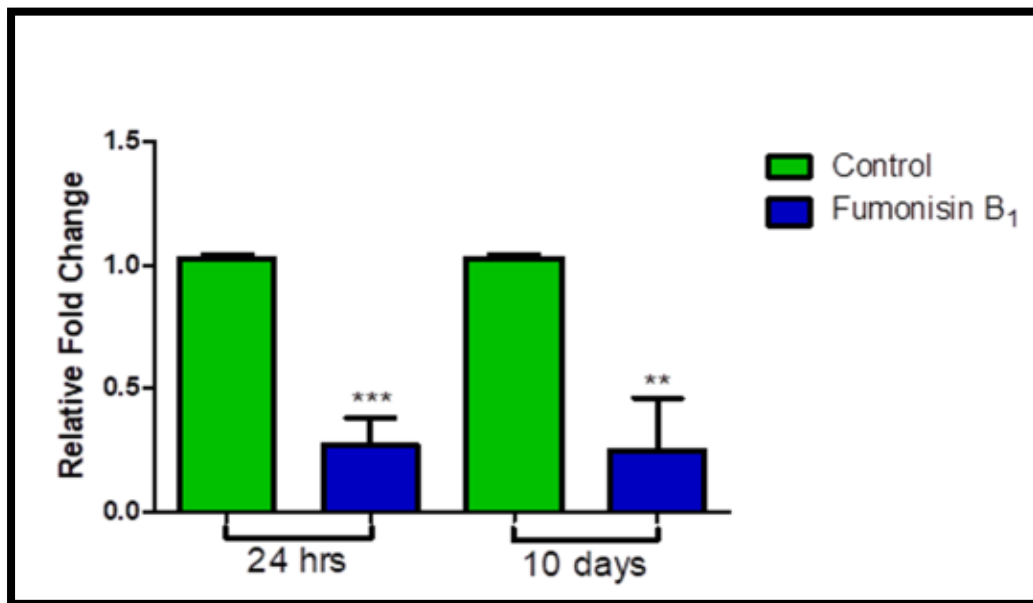


Figure 4.3: mRNA levels of *Nrf2* in C57BL/6 mice brain exposed to FB₁ for 24hrs (*** $p=0,0001$) and 10 days (** $p=0,0013$).

4.2.2 Post transcriptional regulation of Nrf2

MiR-141 inhibits the Keap1-Nrf2 interaction, resulting in Nrf2 being activated and directed into the nucleus instead of being degraded by the proteasome. Using qPCR it was determined that FB₁ induced a significant decrease in *miR-141* levels in mice brain following acute (24hrs: ** $p=0,0019$; Figure 4.4) and prolonged (10 days: *** $p=0,0004$; Figure 4.4) exposure.

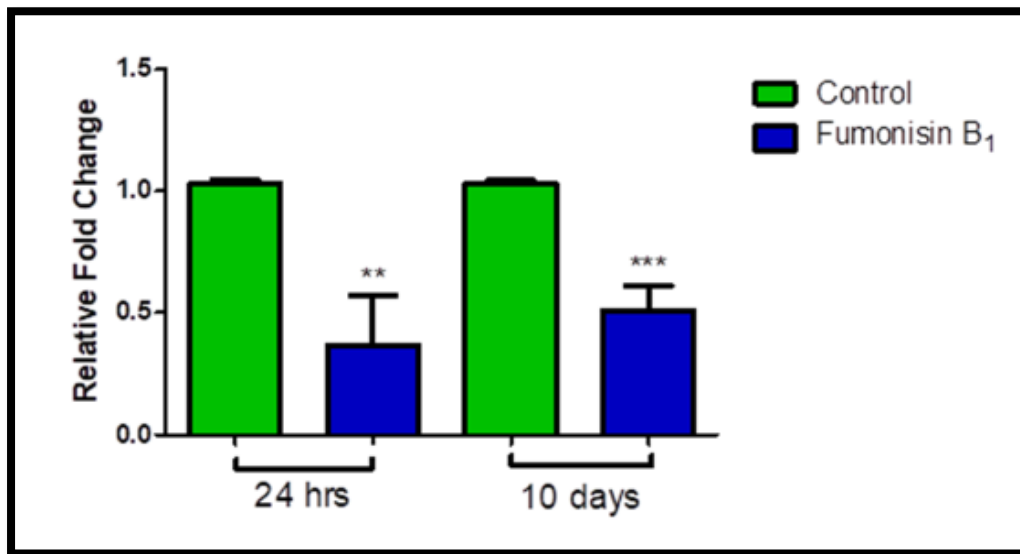


Figure 4.4: *MiR-141* expression in C57BL/6 mice brain exposed to FB₁ for 24 hrs (** $p=0,0019$) and 10 days (*** $p=0,0004$).

4.2.2 Superoxide detoxification

SOD2 converts toxic superoxide, a by-product of the mitochondrial electron transport chain, into hydrogen peroxide and diatomic oxygen. *SOD2* mRNA expression was investigated using qPCR. The results indicate that FB₁ significantly decreased the mRNA expression of *SOD2* in mice brain following acute (24hrs: ** $p= 0,0070$; Figure 4.5) and non-significantly decrease upon prolonged (10 days: $p=0,2725$; Figure 4.5) exposure.

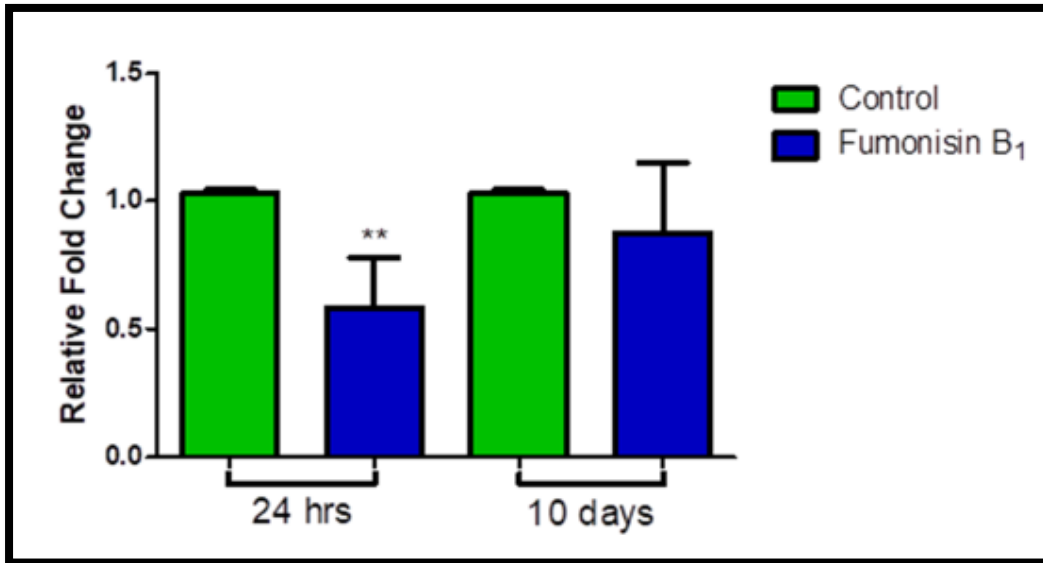


Figure 4.5: mRNA levels of *SOD2* in C57BL/6 mice brain exposed to FB₁ for 24 hrs (** $p= 0,0070$) and 10 days ($p= 0,2725$).

4.2.3 Detoxification of peroxides

GPx protects against oxidative damage by reducing free hydrogen peroxide to water. FB_1 significantly increased the mRNA expression of *GPx* in acute (24hrs: *** $p=0,0001$; Figure 4.6) and prolonged (10 days: ** $p=0,0024$); Figure 4.6) exposure.

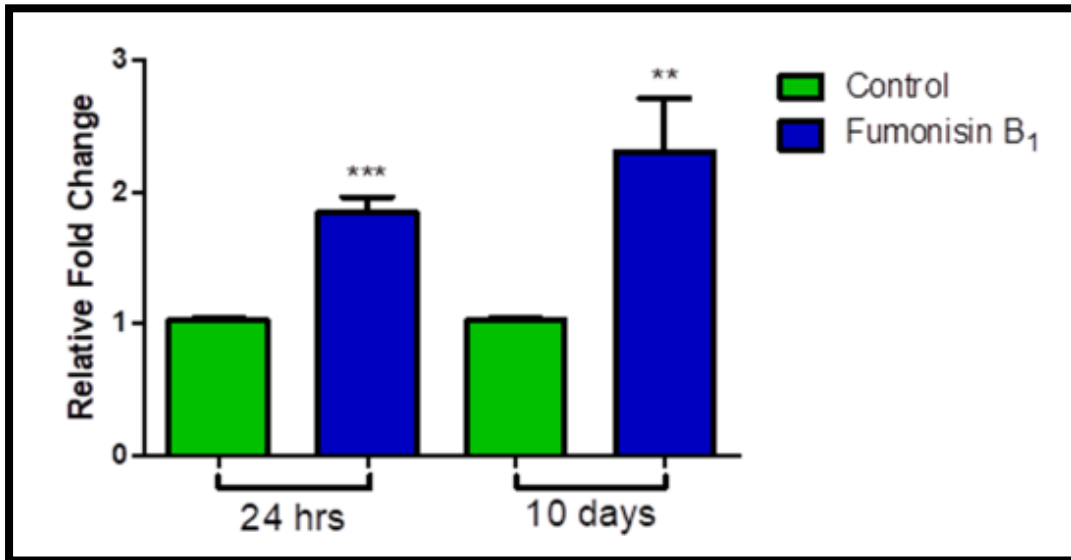


Figure 4.6: mRNA levels of *GPx* in C57BL/6 mice brain exposed to FB_1 for 24 hrs (*** $p=0,0001$) and 10 days (** $p=0,0024$).

4.2.4 Mitochondrial stress response

Tfam is the transcription factor responsible for mitochondrial DNA stabilization. *Tfam* mRNA levels were significantly decreased upon acute (24hrs: *** $p=0,0003$; Figure 4.7) and prolonged (10 days: * $p=0,0196$; Figure 4.7) exposure to FB₁.

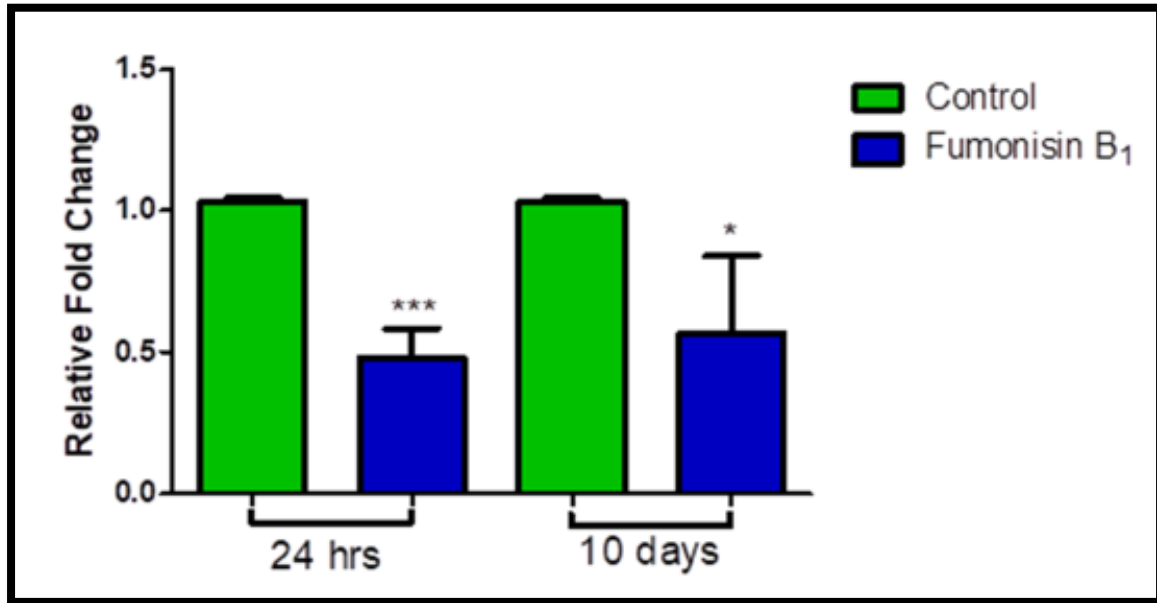


Figure 4.7: mRNA levels of *Tfam* in C57BL/6 mice brain exposed to FB₁ for 24 hrs (***) $p=0,0003$) and 10 days (* $p=0,0196$).

Mitochondrial stress response protein, LONP1 is induced during oxidative and mitochondrial stress. FB₁ significantly decreased the mRNA expression of *LONP1* upon acute (24hrs: *** $p=0,0005$; Figure 4.8) and prolonged (10 days: * $p=0,0117$; Figure 4.8) exposure.

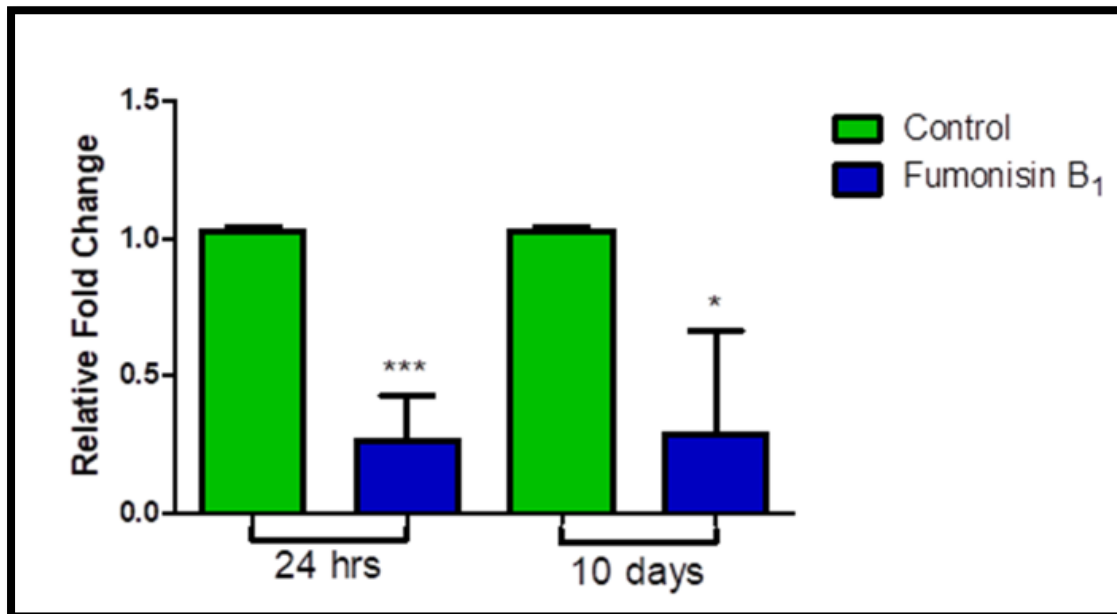


Figure 4.8: mRNA levels of *LONP1* in C57BL/6 mice brain exposed to FB₁ for 24 hrs (** $p=0,0005$) and 10 days (* $p=0,0117$).

The mitochondrial stress response gene, *SIRT3*, is highly expressed during oxidative and mitochondrial stress. The expression of *SIRT3* mRNA was decreased upon acute (24hrs: $p= 0,0594$; Figure 4.9) exposure to FB_1 and significantly increased upon prolonged (10 days: $*p= 0,0283$; Figure 4.9) exposure to FB_1 .

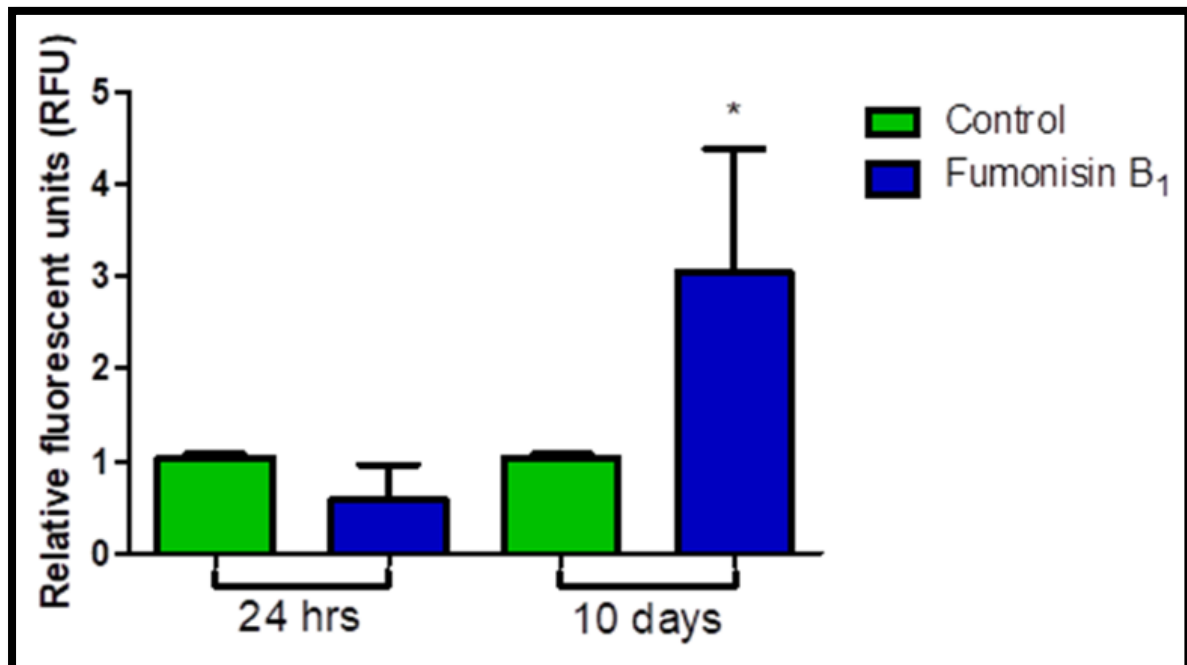


Figure 4.9: mRNA levels of *SIRT3* in C57BL/6 mice brain exposed to FB_1 for 24 hrs ($p= 0,0594$) and 10 days ($*p= 0,0283$).

4.2.5 Expression of neuronal disease related genes

The *tau* gene regulates self-assembly of tangles of paired helical filaments and straight filaments, which are involved in the pathogenesis of Alzheimer's disease and other tauopathies. The mRNA expression of *tau* was significantly reduced upon acute (24hrs: $**p=0,0054$; Figure 4.10) and prolonged (10 days: $*p= 0,0273$; Figure 4.10) exposure to FB₁.

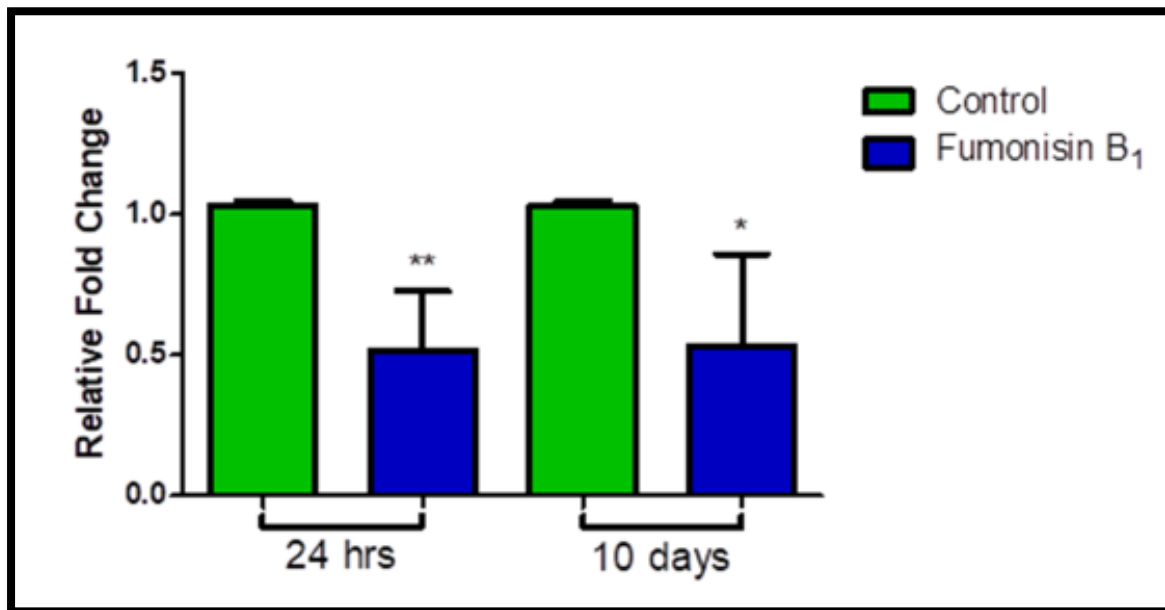


Figure 4.10: mRNA levels of *Tau* in C57BL/6 mice brain exposed to FB₁ for 24 hrs ($**p= 0,0054$) and 10 days ($*p= 0,0273$).

Chapter 5 – Discussion

The mycotoxin, FB₁ is a 2B carcinogenic product of ubiquitous soil fungi *F. verticilloides* and *F. proliferatum*. It is a common contaminant of maize and maize-based products (Marasas 2001, Chaturgoon, Phulukdaree et al. 2015). FB₁ can enter the brain by passing through the blood-brain barrier due to its high polarity and small size (Bezuidenhout, Gelderblom et al. 1988). Neurodegenerative disorders such as AD has been attributed in part to increased oxidative damage to DNA, of which mitochondrial DNA is particularly sensitive to oxidative damage (Mecocci, MacGarvey et al. 1994), since mitochondrial DNA lacks protective histone packaging and mitochondrial ETC generates ROS as a by-product during energy production (Gao, Laude et al. 2008).

Mitochondrial health is imperative to the brain as this impacts energy output and redox status. The mitochondria's principal function is to generate ATP through the ETC. Although low concentrations of ROS are important for normal physiological functions like gene expression, cellular growth and defence against infection (López-Alarcón and Denicola 2013), the excessive production of ROS can have several negative effects. Abnormal production of ROS from the ETC can be caused by inhibition of complex I of the ETC (Bratic and Larsson 2013). Previously, it was reported that FB₁ inhibited complex I of the ETC, thus inducing excessive ROS production and mitochondrial depolarisation, and advancing the oxidative environment (Domijan and Abramov 2011). After incubation of SH-SY5Y cells with FB₁, Domijan and Abramov observed significantly high levels of ROS (Domijan and Abramov 2011).

FB₁ promotes the production of free radical intermediates and accelerates chain reactions associated with lipid peroxidation which results in FB₁-induced injury (Yin, Smith et al. 1998, Lemmer, Gelderblom et al. 1999). This is in accordance with other studies conducted both *in vivo* and *in vitro* (Kouadio, Mobio et al. 2005, Bernabucci, Colavecchia et al. 2011, Wang, Wu et al. 2016).

ROS such as hydrogen peroxide and hydroxyl radicals were reported to be involved in nucleic acid and protein oxidation in rat spleen mononuclear cells following a 48 hr exposure with FB₁ (Mary, Theumer et al. 2012). FB₁ also downregulates the base excision repair gene, 8-Oxoguanine glycosylase (*OGG1*), in oesophageal cancer cells (Khan, Phulukdaree et al. 2018) suggesting that OGG1 would not be able to reduce DNA damage under oxidative conditions.

Redox homeostasis is dependent on the disassociation of the antioxidant transcription factor, Nrf2, from its inhibitor Keap1. MiR-141 functions in the regulation of Keap1 expression at the posttranscriptional level (Eades, Yang et al. 2011). The TargetScan5.1 prediction algorithm identified one conserved miRNA targeting site within the *Keap1* mRNA 3'-UTR, a site complementary to miR-200a and miR-

141 (which share identical seed sequences) (Eades, Yang et al. 2011). MiR-141 targets the 3' UTR of Keap1 (Eades, Yang et al. 2011), inhibiting the interaction between Keap1 and Nrf2. The significant reduction in the expression of miR-141 (Figure 4.4) after acute and prolonged exposure of mice brain to FB₁ implies that the Keap1-Nrf2 complex remained intact and Nrf2 was significantly reduced. This was confirmed in our study in which the expression of total Nrf2 protein was significantly increased upon 24hr exposure to FB₁ and significantly reduced upon 10 days exposure (Figure 4.1), whereas the mRNA expression of *Nrf2* was significantly decreased at both 24 hrs and 10 days (Figure 4.3). The phosphorylation of Nrf2 on serine 40 has been associated with an increase in Nrf2 stability and activity. The expression of pNrf2 on serine 40 was significantly increased following acute exposure and decreased following prolonged exposure to FB₁ (Figure 4.1). This implies that despite the increased expression of Nrf2 and pNrf2 upon 24hr FB₁ exposure, ROS persisted, as indicated by the significant reduction in both the mRNA and protein expression of Nrf2 upon 10 days exposure to FB₁.

Downregulation of Nrf2 affected the response of enzymatic antioxidants. Radical scavenging mechanisms consist of 3 major antioxidant enzymes namely, SOD, CAT and GPx that are regulated by Nrf2. These antioxidants are the first to respond to abnormal levels of ROS. Superoxide dismutase acts as the first line of defence, catalysing the conversion of O₂⁻ to H₂O₂, while CAT and GPx further detoxify H₂O₂ to H₂O and O₂ (Krinsky 1992, Wang, Wu et al. 2016). Inhibition of complex I of ETC by FB₁ induces the production of ROS (Bratic and Larsson 2013). SOD2, CAT and GPx work in concert to detoxify ROS products (Krinsky 1992, Wang, Wu et al. 2016). The expression of *SOD2* was significantly downregulated in C57BL/6 mice brain after exposure to FB₁ (Figure 4.5), while the expression of CAT and GPx were upregulated in mice brain upon exposure to FB₁ (Figure 4.2 and Figure 4.6, respectively). The reduction of *SOD2* mRNA expression in mice brain is in agreement with other studies that noted a its reduction in Balb/c mice and peripheral blood mononuclear cells (PBMC) exposed to FB₁ (Bernabucci, Colavecchia et al. 2011, Abbas, Ben Salah-Abbès et al. 2016). The reduction of *SOD2* gene expression at 24hr and 10 days of exposure to FB₁, might be considered as the result of the well-known inhibitory effect of some mycotoxins on the synthesis of RNA and proteins (Eriksen, Pettersson et al. 2004). Upregulation of CAT protein after exposure to FB₁, is not enough to bring ROS homeostasis when SOD2 is downregulated, Hence SOD2 functions to convert O₂⁻ to H₂O₂. When H₂O₂ is left unconverted, it is converted to OH⁻, resulting in further oxidative damage. *GPx* mRNA, was significantly upregulated after exposure to FB₁ upon 24 hrs and 10 days with reduced activity without SOD2 aid in ROS elimination.

It has been demonstrated that FB₁ targets the mitochondria, nucleus and nucleolus (Myburg, Needhi et al. 2009). Mitochondrial DNA is highly vulnerable to oxidative damage since it lacks protective histone packaging and is in close proximity to the ETC (Gao, Laude et al. 2008). DNA complexes in the mitochondria may resemble those in their bacterial ancestors (Bogenhagen, Wang et al. 2003). The

mtDNA prevents damage by oxidative stress by organising within the nucleoid. Nucleoid components are regulated by the transcription factor, Tfam (Gilkerson, Bravo et al. 2013). Tfam is one of the regulators of transcription of genes encoded by mtDNA and controls mtDNA copy number (Rantanen, Jansson et al. 2001, Noack, Bednarek et al. 2006). Tfam has the ability to bind non-specifically to DNA, which is advantageous since Tfam protects mtDNA by binding directly to the whole genome (Kanki, Ohgaki et al. 2004). The significant downregulation of *Tfam* mRNA expression (Figure 4.7) in mice brain after exposure to FB₁ for 24hrs and 10 days may be an indication of compromised mtDNA replication, leading to mutations, which may result to cancer and neurodegeneration.

Although phosphorylation of Tfam was not measure in this study, from literature it has been reported that FB₁ activates extracellular signal-regulated kinases (ERK) cascades, which is involved in Tfam phosphorylation (Rumora, Domijan et al. 2007, Lu, Lee et al. 2013). Phosphorylated Tfam cannot bind to mtDNA and is incapable of protecting mtDNA, leaving it vulnerable to ROS-induced insults and genome instability. Phosphorylation of Tfam results in its rapid degradation by LONP1, a primary mitochondrial protease which also regulates mtDNA copy number and transcription (Bota and Davies 2016). The significant downregulation of *LONP1* mRNA expression following exposure to FB₁ (Figure 4.8), indicates increased mitochondrial stress and loss of mitochondrial integrity (Ngo, Pomatto et al. 2013).

SIRT3, a mitochondrial deacetylase enzyme, is responsible for activation of LONP1 at the post-transcriptional level (Bota and Davies 2016). SIRT3 was downregulated after 24hr exposure, but significantly upregulated upon 10 days exposure to FB₁ (Figure 4.9). SIRT3 is NAD⁺ dependent, hence it acts as an energy sensor in the mitochondria. The requirement of co-factor NAD⁺ by SIRT3 for the deacetylase activity, places SIRT3 at the centre of energy metabolism in the mitochondria (Nogueiras, Habegger et al. 2012). Compromised mitochondria will reduce ATP production, so ATP-dependent mechanisms are compromised, such as LONP1 regulation. Furthermore, decreased SOD2 activity reduces the detoxification capacity of the mitochondria (Bause and Haigis 2013).

Abnormal tau expression and oxidative stress have been implicated as important pathogenetic events in tauopathies including Alzheimer's disease (AD) (Cente, Filipcik et al. 2006). Human truncated variant form of tau protein leads to the accumulation of ROS and sensitizes rat cortical neurons to cell death induced by oxidative stress (Cente, Filipcik et al. 2006). The *Tau* mRNA was significantly downregulated at 24hr and 10 days exposure to FB₁ (Figure 10). The loss of normal tau MT-stabilizing function has been reported to lead to a pathological disturbance in the normal structural and regulatory functions of the cytoskeleton, compromising axonal transport and thus contributes to synaptic dysfunction and neurodegeneration (Ballatore, Lee et al. 2007). Nrf2 activation promotes the

degradation of tau protein, indicating that the reduction in *Tau* expression contributes to ROS-induced damage in mice brain (Jo, Gundemir et al. 2014).

Exposure to FB₁ generated oxidative stress in mice brain, inducing mitochondrial and antioxidant responses to reduce increased ROS levels. These responses were compromised leading to mitochondrial dysfunction and neurodegeneration. However, further research needs to be conducted to determine the role of ROS and Nrf2 in FB₁ induced neurodegeneration.

5.1 Limitations and Future studies

The limitation of this study was that ROS was not directly tested. In future it will be much better to develop/find novel protocols to measure ROS *in vivo*. Another interesting area to make this study even better, is to conduct gene knockouts and observe the antioxidant response in mice after exposure to FB₁.

5.2 Conclusion

This study provided evidence that exposing mice brain to FB₁ upon 24hrs and 10 days, alters antioxidant processes. Compromised antioxidant capacity may not have the ability to deal with the excessive ROS, which may result from exposure to FB₁. Furthermore, mitochondrial survival responses were also compromised (downregulated SOD2, Tfam and LONP1), inducing mitochondrial stress. Hence, the excessive ROS induced by FB₁, and compromised survival responses may be implicated in FB₁ neurodegeneration (downregulated Tau, hence AD).

References

- Abbax, H., et al. (1993). "Biological activities of fumonisins, mycotoxins from *Fusarium moniliforme*, in jimsonweed (*Datura stramonium* L.) and mammalian cell cultures." Toxicon **31**(3): 345-353.
- Abbes, S., et al. (2016). "Interaction of aflatoxin B1 and fumonisin B1 in mice causes immunotoxicity and oxidative stress: Possible protective role using lactic acid bacteria." Journal of immunotoxicology **13**(1): 46-54.
- Arya, M., et al. (2005). "Basic principles of real-time quantitative PCR." Expert review of molecular diagnostics **5**(2): 209-219.

- Baek, B. S., et al. (1999). "Regional difference of ROS generation, lipid peroxidation, and antioxidant enzyme activity in rat brain and their dietary modulation." Archives of pharmacological research **22**(4): 361.
- Ballatore, C., et al. (2007). "Tau-mediated neurodegeneration in Alzheimer's disease and related disorders." Nature Reviews Neuroscience **8**(9): 663.
- Bause, A. S. and M. C. Haigis (2013). "SIRT3 regulation of mitochondrial oxidative stress." Experimental gerontology **48**(7): 634-639.
- Bayr, H. (2005). "Reactive oxygen species." Critical care medicine **33**(12): S498-S501.
- Becuwe, P., et al. (2014). "Manganese superoxide dismutase in breast cancer: from molecular mechanisms of gene regulation to biological and clinical significance." Free Radical Biology and Medicine **77**: 139-151.
- Bernabucci, U., et al. (2011). "Aflatoxin B1 and fumonisin B1 affect the oxidative status of bovine peripheral blood mononuclear cells." Toxicology in vitro **25**(3): 684-691.
- Bezuidenhout, S. C., et al. (1988). "Structure elucidation of the fumonisins, mycotoxins from *Fusarium moniliforme*." Journal of the Chemical Society, Chemical Communications(11): 743-745.
- Bhat, R. V., et al. (1997). "A foodborne disease outbreak due to the consumption of moldy sorghum and maize containing fumonisin mycotoxins." Journal of Toxicology: Clinical Toxicology **35**(3): 249-255.
- Birben, E., et al. (2012). "Oxidative stress and antioxidant defense." World Allergy Organization Journal **5**(1): 9.
- Bogenhagen, D. F., et al. (2003). "Protein components of mitochondrial DNA nucleoids in higher eukaryotes." Molecular & Cellular Proteomics **2**(11): 1205-1216.
- Bota, D. A. and K. J. Davies (2016). "Mitochondrial Lon protease in human disease and aging: Including an etiologic classification of Lon-related diseases and disorders." Free Radical Biology and Medicine **100**: 188-198.
- Bratic, A. and N.-G. Larsson (2013). "The role of mitochondria in aging." The Journal of clinical investigation **123**(3): 951-957.
- Brownie, C. and J. Cullen (1987). "Characterization of experimentally induced equine leukoencephalomalacia (ELEM) in ponies (*Equus caballus*): preliminary report." Veterinary and human toxicology **29**(1): 34-38.

- Bucci, T. J., et al. (1996). "Leukoencephalomalacia and hemorrhage in the brain of rabbits gavaged with mycotoxin fumonisin B1." Natural Toxins **4**(1): 51-52.
- Buetler, T. M., et al. (1995). "Induction of phase I and phase II drug-metabolizing enzyme mRNA, protein, and activity by BHA, ethoxyquin, and oltipraz." Toxicology and applied pharmacology **135**(1): 45-57.
- Cente, M., et al. (2006). "Expression of a truncated tau protein induces oxidative stress in a rodent model of tauopathy." European Journal of Neuroscience **24**(4): 1085-1090.
- Chen, Q., et al. (2014). "MicroRNA-23a/b and microRNA-27a/b suppress Apaf-1 protein and alleviate hypoxia-induced neuronal apoptosis." Cell death & disease **5**(3): e1132.
- Cheng, A., et al. (2016). "Mitochondrial SIRT3 mediates adaptive responses of neurons to exercise and metabolic and excitatory challenges." Cell metabolism **23**(1): 128-142.
- Chu, F. S. and G. Y. Li (1994). "Simultaneous occurrence of fumonisin B1 and other mycotoxins in moldy corn collected from the People's Republic of China in regions with high incidences of esophageal cancer." Applied and environmental microbiology **60**(3): 847-852.
- Chuturgoon, A. A., et al. (2014). "Fumonisin B1 modulates expression of human cytochrome P450 1b1 in human hepatoma (Hepg2) cells by repressing Mir-27b." Toxicology letters **227**(1): 50-55.
- Chuturgoon, A. A., et al. (2015). "Fumonisin B1 inhibits apoptosis in HepG2 cells by inducing Birc-8/ILP-2." Toxicology letters **235**(2): 67-74.
- Chuturgoon, A., et al. (2014). "Fumonisin B1 induces global DNA hypomethylation in HepG2 cells—An alternative mechanism of action." Toxicology **315**: 65-69.
- Cogswell, J. P., et al. (2008). "Identification of miRNA changes in Alzheimer's disease brain and CSF yields putative biomarkers and insights into disease pathways." Journal of Alzheimer's disease **14**(1): 27-41.
- Coulombe Jr, R. A. (1993). "Biological Action of Mycotoxins I." Journal of dairy science **76**(3): 880-891.
- Creppy, E. E. (2002). "Update of survey, regulation and toxic effects of mycotoxins in Europe." Toxicology letters **127**(1-3): 19-28.
- da Rocha, M. E. B., et al. (2014). "Mycotoxins and their effects on human and animal health." Food Control **36**(1): 159-165.

- Detrait, E. R., et al. (2005). "Human neural tube defects: developmental biology, epidemiology, and genetics." Neurotoxicology and teratology **27**(3): 515-524.
- Domijan, A.-M. and A. Y. Abramov (2011). "Fumonisin B1 inhibits mitochondrial respiration and deregulates calcium homeostasis—implication to mechanism of cell toxicity." The international journal of biochemistry & cell biology **43**(6): 897-904.
- Dragan, Y. P., et al. (2001). "Implications of apoptosis for toxicity, carcinogenicity, and risk assessment: fumonisin B1 as an example." Toxicological Sciences **61**(1): 6-17.
- Eades, G., et al. (2011). "miR-200a regulates Nrf2 activation by targeting Keap1 mRNA in breast cancer cells." Journal of Biological Chemistry: jbc. M111. 275495.
- Egger, A. L., et al. (2008). "Molecular mechanisms of natural products in chemoprevention: induction of cytoprotective enzymes by Nrf2." Molecular nutrition & food research **52**(S1).
- Eriksen, G. S., et al. (2004). "Comparative cytotoxicity of deoxynivalenol, nivalenol, their acetylated derivatives and de-epoxy metabolites." Food and Chemical Toxicology **42**(4): 619-624.
- Escrivá, H., et al. (1999). "Expression of mitochondrial genes and of the transcription factors involved in the biogenesis of mitochondria Tfam, NRF-1 and NRF-2, in rat liver, testis and brain." Biochimie **81**(10): 965-971.
- Eslami, A. and J. Lujan (2010). "Western blotting: sample preparation to detection." Journal of visualized experiments: JoVE(44).
- Fernandez-Surumay, G., et al. (2005). "Fumonisin B– Glucose Reaction Products Are Less Toxic When Fed to Swine." Journal of Agricultural and Food Chemistry **53**(10): 4264-4271.
- Fincham, J., et al. (1992). "Atherogenic effects in a non-human primate of Fusarium moniliforme cultures added to a carbohydrate diet." Atherosclerosis **94**(1): 13-25.
- Franceschi, S., et al. (1990). "Maize and risk of cancers of the oral cavity, pharynx, and esophagus in northeastern Italy." JNCI: Journal of the National Cancer Institute **82**(17): 1407-1411.
- Friling, R. S., et al. (1990). "Xenobiotic-inducible expression of murine glutathione S-transferase Ya subunit gene is controlled by an electrophile-responsive element." Proceedings of the National Academy of Sciences **87**(16): 6258-6262.
- Galvano, F., et al. (2001). "Dietary strategies to counteract the effects of mycotoxins: a review." Journal of food protection **64**(1): 120-131.

- Gao, L., et al. (2008). "Mitochondrial pathophysiology, reactive oxygen species, and cardiovascular diseases." Veterinary Clinics of North America: Small Animal Practice **38**(1): 137-155.
- Gelderblom, W. and W. Marasas (2012). "Controversies in fumonisin mycotoxicology and risk assessment." Human & experimental toxicology **31**(3): 215-235.
- Gelderblom, W. C., et al. (1991). "Toxicity and carcinogenicity of the Fusarium moniliforme metabolite, fumonisin B1, in rats." Carcinogenesis **12**(7): 1247-1251.
- Gelderblom, W. C., et al. (1992). "Fumonisin: isolation, chemical characterization and biological effects." Mycopathologia **117**(1-2): 11-16.
- Gelderblom, W., et al. (1988). "Fumonisin--novel mycotoxins with cancer-promoting activity produced by Fusarium moniliforme." Applied and environmental microbiology **54**(7): 1806-1811.
- Gelderblom, W., et al. (1993). "Structure-activity relationships of fumonisins in short-term carcinogenesis and cytotoxicity assays." Food and Chemical Toxicology **31**(6): 407-414.
- Gibellini, L., et al. (2014). "Sirtuin 3 interacts with Lon protease and regulates its acetylation status." Mitochondrion **18**: 76-81.
- Gilkerson, R., et al. (2013). "The mitochondrial nucleoid: integrating mitochondrial DNA into cellular homeostasis." Cold Spring Harbor perspectives in biology **5**(5): a011080.
- Groves, F. D., et al. (1999). "Fusarium mycotoxins in corn and corn products in a high-risk area for gastric cancer in Shandong Province, China." Journal of AOAC International **82**(3): 657-662.
- Hansen, J. M., et al. (2004). "Compartmentation of Nrf-2 redox control: regulation of cytoplasmic activation by glutathione and DNA binding by thioredoxin-1." Toxicological Sciences **82**(1): 308-317.
- Harel, R. and A. Futerman (1993). "Inhibition of sphingolipid synthesis affects axonal outgrowth in cultured hippocampal neurons." Journal of Biological Chemistry **268**(19): 14476-14481.
- Harrison, L. R., et al. (1990). "Pulmonary edema and hydrothorax in swine produced by fumonisin B1, a toxic metabolite of Fusarium moniliforme." Journal of Veterinary Diagnostic Investigation **2**(3): 217-221.

- Hayes, J. D. and D. J. Pulford (1995). "The glutathione S-transferase supergene family: regulation of GST and the contribution of the isoenzymes to cancer chemoprotection and drug resistance part II." Critical reviews in biochemistry and molecular biology **30**(6): 521-600.
- He, L. and G. J. Hannon (2004). "MicroRNAs: small RNAs with a big role in gene regulation." Nature Reviews Genetics **5**(7): 522.
- He, W., et al. (2012). "Mitochondrial sirtuins: regulators of protein acylation and metabolism." Trends in Endocrinology & Metabolism **23**(9): 467-476.
- Huang, H.-C., et al. (2002). "Phosphorylation of Nrf2 at Ser40 by protein kinase C regulates antioxidant response element-mediated transcription." Journal of Biological Chemistry.
- Huang, T., et al. (2010). "Competitive binding to cuprous ions of protein and BCA in the bicinchoninic acid protein assay." The open biomedical engineering journal **4**: 271.
- Huang, Y., et al. (2015). "The complexity of the Nrf2 pathway: beyond the antioxidant response." The Journal of nutritional biochemistry **26**(12): 1401-1413.
- Humpf, H. U. and K. A. Voss (2004). "Effects of thermal food processing on the chemical structure and toxicity of fumonisin mycotoxins." Molecular nutrition & food research **48**(4): 255-269.
- Hussein, H. S. and J. M. Brasel (2001). "Toxicity, metabolism, and impact of mycotoxins on humans and animals." Toxicology **167**(2): 101-134.
- Ishii, T., et al. (2000). "Transcription factor Nrf2 coordinately regulates a group of oxidative stress-inducible genes in macrophages." Journal of Biological Chemistry **275**(21): 16023-16029.
- Itoh, K., et al. (1995). "Cloning and characterization of a novel erythroid cell-derived CNC family transcription factor heterodimerizing with the small Maf family proteins." Molecular and cellular biology **15**(8): 4184-4193.
- Itoh, K., et al. (1999). "Keap1 represses nuclear activation of antioxidant responsive elements by Nrf2 through binding to the amino-terminal Neh2 domain." Genes & development **13**(1): 76-86.
- Itoh, K., et al. (2003). "Keap1 regulates both cytoplasmic-nuclear shuttling and degradation of Nrf2 in response to electrophiles." Genes to Cells **8**(4): 379-391.
- Jo, C., et al. (2014). "Nrf2 reduces levels of phosphorylated tau protein by inducing autophagy adaptor protein NDP52." Nature communications **5**: 3496.

- Jones, D. P. (2006). "Redefining oxidative stress." Antioxidants & redox signaling **8**(9-10): 1865-1879.
- Kanki, T., et al. (2004). "Architectural role of mitochondrial transcription factor A in maintenance of human mitochondrial DNA." Molecular and cellular biology **24**(22): 9823-9834.
- Khan, R., et al. (2018). "Concentration-dependent effect of fumonisin B1 on apoptosis in oesophageal cancer cells." Human & experimental toxicology **37**(7): 762-771.
- Kouadio, J. H., et al. (2005). "Comparative study of cytotoxicity and oxidative stress induced by deoxynivalenol, zearalenone or fumonisin B1 in human intestinal cell line Caco-2." Toxicology **213**(1-2): 56-65.
- Kriek, N., et al. (1981). "A comparative study of the toxicity of *Fusarium verticillioides* (= *F. moniliforme*) to horses, primates, pigs, sheep and rats." The Onderstepoort journal of veterinary research **48**(2): 129-131.
- Krinsky, N. I. (1992). "Mechanism of action of biological antioxidants." Proceedings of the Society for Experimental Biology and Medicine **200**(2): 248-254.
- Krska, R., et al. (2007). "Analysis of *Fusarium* toxins in feed." Animal Feed Science and Technology **137**(3-4): 241-264.
- Kwon, O.-S., et al. (2000). "Biochemical and morphological effects of fumonisin B1 on primary cultures of rat cerebrum." Neurotoxicology and teratology **22**(4): 565-572.
- Lemmer, E. R., et al. (1999). "The effects of dietary iron overload on fumonisin B1-induced cancer promotion in the rat liver." Cancer letters **146**(2): 207-215.
- Li, W. and A. N. Kong (2009). "Molecular mechanisms of Nrf2-mediated antioxidant response." Molecular carcinogenesis **48**(2): 91-104.
- Li, Y., et al. (1999). "Effects of fumonisin B1 on selected immune responses in broiler chicks." Poultry science **78**(9): 1275-1282.
- Liu, H., et al. (2015). "Role of SIRT3 in Angiotensin II-induced human umbilical vein endothelial cells dysfunction." BMC cardiovascular disorders **15**(1): 81.
- Livak, K. J. and T. D. Schmittgen (2001). "Analysis of relative gene expression data using real-time quantitative PCR and the 2⁻ ΔΔCT method." methods **25**(4): 402-408.
- Lobo, V., et al. (2010). "Free radicals, antioxidants and functional foods: Impact on human health." Pharmacognosy reviews **4**(8): 118.

- López-Alarcón, C. and A. Denicola (2013). "Evaluating the antioxidant capacity of natural products: A review on chemical and cellular-based assays." Analytica chimica acta **763**: 1-10.
- Lu, B., et al. (2013). "Phosphorylation of human TFAM in mitochondria impairs DNA binding and promotes degradation by the AAA+ Lon protease." Molecular cell **49**(1): 121-132.
- Mahmood, T. and P.-C. Yang (2012). "Western blot: technique, theory, and trouble shooting." North American journal of medical sciences **4**(9): 429.
- Malhotra, B. D., et al. (2014). "Nanomaterial-based biosensors for food toxin detection." Applied biochemistry and biotechnology **174**(3): 880-896.
- Marasas, W. (2001). "Discovery and occurrence of the fumonisins: a historical perspective." Environmental health perspectives **109**(Suppl 2): 239.
- Marasas, W. F. O., et al. (2014). "Leukoencephalomalacia in a horse induced by fumonisin B₁ isolated from *Fusarium moniliforme*."
- Marasas, W. F., et al. (2004). "Fumonisins disrupt sphingolipid metabolism, folate transport, and neural tube development in embryo culture and in vivo: a potential risk factor for human neural tube defects among populations consuming fumonisin-contaminated maize." The Journal of nutrition **134**(4): 711-716.
- Markesbery, W. R. (1997). "Oxidative stress hypothesis in Alzheimer's disease." Free Radical Biology and Medicine **23**(1): 134-147.
- Martinova, E. A. and A. H. Merrill (1995). "Fumonisin B₁ alters sphingolipid metabolism and immune function in BALB/c mice: Immunological responses to fumonisin B₁." Mycopathologia **130**(3): 163-170.
- Mary, V. S., et al. (2012). "Reactive oxygen species sources and biomolecular oxidative damage induced by aflatoxin B₁ and fumonisin B₁ in rat spleen mononuclear cells." Toxicology **302**(2-3): 299-307.
- Maslov, L., et al. (2015). "Reactive oxygen species are triggers and mediators of an increase in cardiac tolerance to impact of ischemia-reperfusion." Rossiiskii fiziologicheskii zhurnal imeni IM Sechenova **101**(1): 3-24.
- Matsushima, Y., et al. (2010). "Mitochondrial Lon protease regulates mitochondrial DNA copy number and transcription by selective degradation of mitochondrial transcription factor A (TFAM)." Proceedings of the National Academy of Sciences.

- Mecocci, P., et al. (1994). "Oxidative damage to mitochondrial DNA is increased in Alzheimer's disease." Annals of Neurology: Official Journal of the American Neurological Association and the Child Neurology Society **36**(5): 747-751.
- Meeting, J. F. W. E. C. o. F. A. (2001). Safety evaluation of certain mycotoxins in food, Food & Agriculture Org.
- Merrill Jr, A. H., et al. (2001). "Sphingolipid metabolism: roles in signal transduction and disruption by fumonisins." Environmental health perspectives **109**(Suppl 2): 283.
- Merrill Jr, A., et al. (1996). "Fumonisin: naturally occurring inhibitors of ceramide synthesis." Journal of Cell Biology.
- Merrill, A., et al. (1993). "Fumonisin B1 inhibits sphingosine (sphinganine) N-acyltransferase and de novo sphingolipid biosynthesis in cultured neurons in situ." Journal of Biological Chemistry **268**(36): 27299-27306.
- Mobio, T. A., et al. (2000). "Epigenetic properties of fumonisin B1: cell cycle arrest and DNA base modification in C6 glioma cells." Toxicology and applied pharmacology **164**(1): 91-96.
- Monnet-Tschudi, F., et al. (1999). "The naturally occurring food mycotoxin fumonisin B1 impairs myelin formation in aggregating brain cell culture." Neurotoxicology **20**(1): 41-48.
- Monnet-Tschudi, F., et al. (2007). "Neurotoxicant-induced inflammatory response in three-dimensional brain cell cultures." Human & experimental toxicology **26**(4): 339-346.
- Musser, S. M. and R. D. Plattner (1997). "Fumonisin composition in cultures of *Fusarium moniliforme*, *Fusarium proliferatum*, and *Fusarium nygami*." Journal of Agricultural and Food Chemistry **45**(4): 1169-1173.
- Myburg, R., et al. (2009). "The ultrastructural effects and immunolocalisation of fumonisin B1 on cultured oesophageal cancer cells (SNO)." South African Journal of Science **105**(5-6): 217-222.
- Ngo, J. K. and K. J. Davies (2009). "Mitochondrial Lon protease is a human stress protein." Free Radical Biology and Medicine **46**(8): 1042-1048.
- Ngo, J. K., et al. (2013). "Upregulation of the mitochondrial Lon Protease allows adaptation to acute oxidative stress but dysregulation is associated with chronic stress, disease, and aging." Redox biology **1**(1): 258-264.

- Nguyen, T., et al. (2003). "Regulatory mechanisms controlling gene expression mediated by the antioxidant response element." Annual review of pharmacology and toxicology **43**(1): 233-260.
- Nguyen, T., et al. (2009). "The Nrf2-antioxidant response element signaling pathway and its activation by oxidative stress." Journal of Biological Chemistry **284**(20): 13291-13295.
- Noack, H., et al. (2006). "TFAM-dependent and independent dynamics of mtDNA levels in C2C12 myoblasts caused by redox stress." Biochimica et Biophysica Acta (BBA)-General Subjects **1760**(2): 141-150.
- Nogueiras, R., et al. (2012). "Sirtuin 1 and sirtuin 3: physiological modulators of metabolism." Physiological reviews **92**(3): 1479-1514.
- Norred, W., et al. (2001). "Instability of N-acetylated fumonisin B1 (FA1) and the impact on inhibition of ceramide synthase in rat liver slices." Food and Chemical Toxicology **39**(11): 1071-1078.
- Omurtag, S. Y. a. G. Z. (2008). "Fumonisin, trichothecenes and zearalenone in cereals." International Journal of Molecular Sciences **9**(11): 2062-2090.
- Onyango, P., et al. (2002). "SIRT3, a human SIR2 homologue, is an NAD-dependent deacetylase localized to mitochondria." Proceedings of the National Academy of Sciences **99**(21): 13653-13658.
- Osuchowski, M. F., et al. (2005). "Fumonisin B1-induced neurodegeneration in mice after intracerebroventricular infusion is concurrent with disruption of sphingolipid metabolism and activation of proinflammatory signaling." Neurotoxicology **26**(2): 211-221.
- Peraica, M., et al. (1999). "Toxic effects of mycotoxins in humans." Bulletin of the World Health Organization **77**(9): 754-766.
- Pestana, E., et al. (2010). Early, rapid and sensitive veterinary molecular diagnostics-real time PCR applications, Springer Science & Business Media.
- Qiu, X., et al. (2010). "Calorie restriction reduces oxidative stress by SIRT3-mediated SOD2 activation." Cell metabolism **12**(6): 662-667.
- Rantanen, A., et al. (2001). "Downregulation of Tfam and mtDNA copy number during mammalian spermatogenesis." Mammalian genome **12**(10): 787-792.
- Rheeder, J., et al. (1992). "Fusarium moniliforme and fumonisins in corn in relation to human esophageal cancer in Transkei."

- Riley, R. T., et al. (1994). "Dietary fumonisin B1 induces disruption of sphingolipid metabolism in Sprague-Dawley rats: a new mechanism of nephrotoxicity." The Journal of nutrition **124**(4): 594-603.
- Riley, R. T., et al. (1997). "Disruption of sphingolipid metabolism and induction of equine leukoencephalomalacia by *Fusarium proliferatum* culture material containing fumonisin B2 or B3." Environmental toxicology and pharmacology **3**(3): 221-228.
- Riley, R. T., et al. (2001). "Sphingolipid perturbations as mechanisms for fumonisin carcinogenesis." Environmental health perspectives **109**(Suppl 2): 301.
- Riley, R., et al. (1993). "Alteration of tissue and serum sphinganine to sphingosine ratio: an early biomarker of exposure to fumonisin-containing feeds in pigs." Toxicology and applied pharmacology **118**(1): 105-112.
- Rumora, L., et al. (2007). "Mycotoxin fumonisin B1 alters cellular redox balance and signalling pathways in rat liver and kidney." Toxicology **242**(1-3): 31-38.
- Rushmore, T. H., et al. (1991). "The antioxidant responsive element. Activation by oxidative stress and identification of the DNA consensus sequence required for functional activity." Journal of Biological Chemistry **266**(18): 11632-11639.
- Sadler, T., et al. (2002). "Prevention of fumonisin B1-induced neural tube defects by folic acid." Teratology **66**(4): 169-176.
- Sahu, S. C., et al. (1998). "Peroxidation of membrane lipids and oxidative DNA damage by fumonisin B1 in isolated rat liver nuclei." Cancer letters **125**(1): 117-121.
- Schmelz, E. M., et al. (1998). "Induction of apoptosis by Fumonisin B1 in HT29 cells is mediated by the accumulation of endogenous free sphingoid bases." Toxicology and applied pharmacology **148**(2): 252-260.
- Scott, P. (2012). "Recent research on fumonisins: a review." Food Additives & Contaminants: Part A **29**(2): 242-248.
- Seo, J.-A. and Y.-W. Lee (1999). "Natural occurrence of the C series of fumonisins in moldy corn." Applied and environmental microbiology **65**(3): 1331-1334.
- Shephard, G. S., et al. (2000). "Natural occurrence of fumonisins in corn from Iran." Journal of Agricultural and Food Chemistry **48**(5): 1860-1864.
- Smith, J. E., et al. (1995). "Role of mycotoxins in human and animal nutrition and health." Natural Toxins **3**(4): 187-192.

- Solst, S. R., et al. (2017). "Inhibition of Mitochondrial Pyruvate Transport Selectively Sensitizes Cancer Cells to Metabolic Oxidative Stress." Free Radical Biology and Medicine **112**: 102.
- Soriano, J., et al. (2005). "Mechanism of action of sphingolipids and their metabolites in the toxicity of fumonisin B1." Progress in lipid research **44**(6): 345-356.
- Stockmann-Juvala, H., et al. (2004). "Oxidative stress induced by fumonisin B1 in continuous human and rodent neural cell cultures." Free radical research **38**(9): 933-942.
- Tao, R., et al. (2010). "Sirt3-mediated deacetylation of evolutionarily conserved lysine 122 regulates MnSOD activity in response to stress." Molecular cell **40**(6): 893-904.
- Tao, R., et al. (2014). "Regulation of MnSOD enzymatic activity by Sirt3 connects the mitochondrial acetylome signaling networks to aging and carcinogenesis." Antioxidants & redox signaling **20**(10): 1646-1654.
- Thiel, P. G., et al. (1992). "The implications of naturally occurring levels of fumonisins in corn for human and animal health." Mycopathologia **117**(1-2): 3-9.
- Walker, J. M. (1996). The protein protocols handbook, Springer Science & Business Media.
- Wang, E., et al. (1992). "Increases in serum sphingosine and sphinganine and decreases in complex sphingolipids in ponies given feed containing fumonisins, mycotoxins produced by *Fusarium moniliforme*." The Journal of nutrition **122**(8): 1706-1716.
- Wang, J., et al. (2016). "Molecular mechanism of catalase activity change under sodium dodecyl sulfate-induced oxidative stress in the mouse primary hepatocytes." Journal of hazardous materials **307**: 173-183.
- Wang, X., et al. (2016). "Fumonisin: oxidative stress-mediated toxicity and metabolism in vivo and in vitro." Archives of toxicology **90**(1): 81-101.
- WHO., J. F. W. E. C. o. F. A. (2001). Safety evaluation of certain mycotoxins in food, Food & Agriculture Org.
- Wu, F., et al. (2014). "Public health impacts of foodborne mycotoxins." Annual review of food science and technology **5**: 351-372.
- Yin, H., et al. (2011). "Free radical lipid peroxidation: mechanisms and analysis." Chemical reviews **111**(10): 5944-5972.
- Yin, J.-J., et al. (1998). "Effects of fumonisin B 1 on lipid peroxidation in membranes." Biochimica et Biophysica Acta (BBA)-Biomembranes **1371**(1): 134-142.

APPENDIX A

NQO1 ensures complete oxidation of quinone substrate without the formation of semiquinones and species with reactive oxygen radicals. FB₁ significantly decreased the mRNA expression of *NQO1* in mice brain following acute (24hrs: ** $p=0,0080$; Figure 6) and non-significant increase upon prolonged (10 days: $p=0,1292$; Figure 6) exposure.

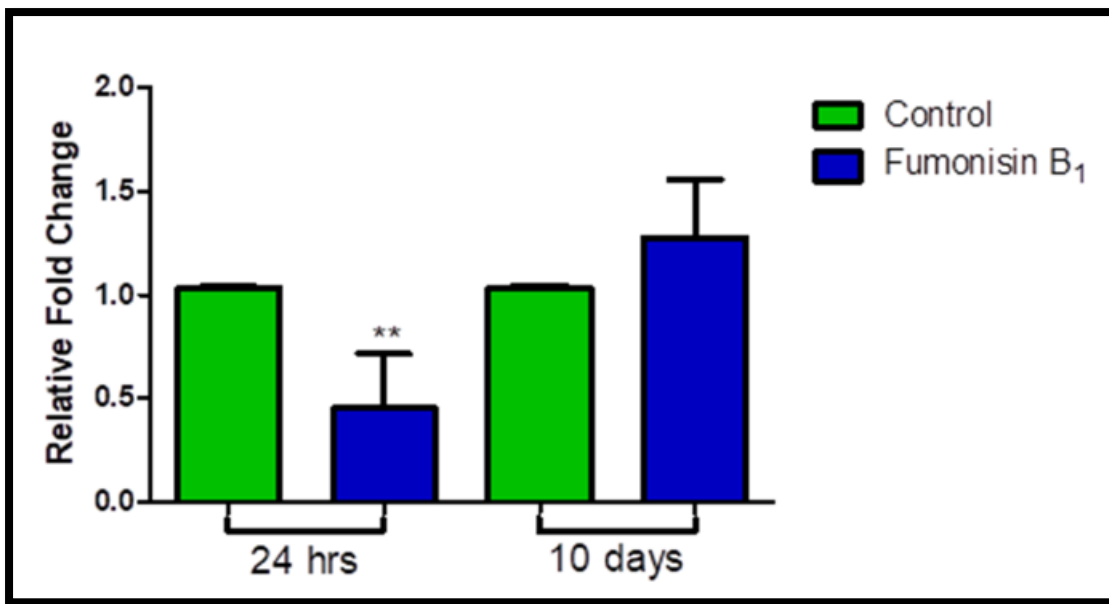


Figure 6: mRNA levels of *NQO1* (24hrs: ** $p=0,0080$; 10 days: $p=0,1292$) in mice brain exposed to FB₁.

APPENDIX B

HO-1 catalyses the degradation of heme and is expressed primarily during oxidative stress. FB₁ significantly decreased the mRNA expression of *HO-1* in mice brain following acute (24hrs: *** p < 0.0001; Figure 7) and prolonged (10 days: *** p < 0.0001; Figure 7) exposure.

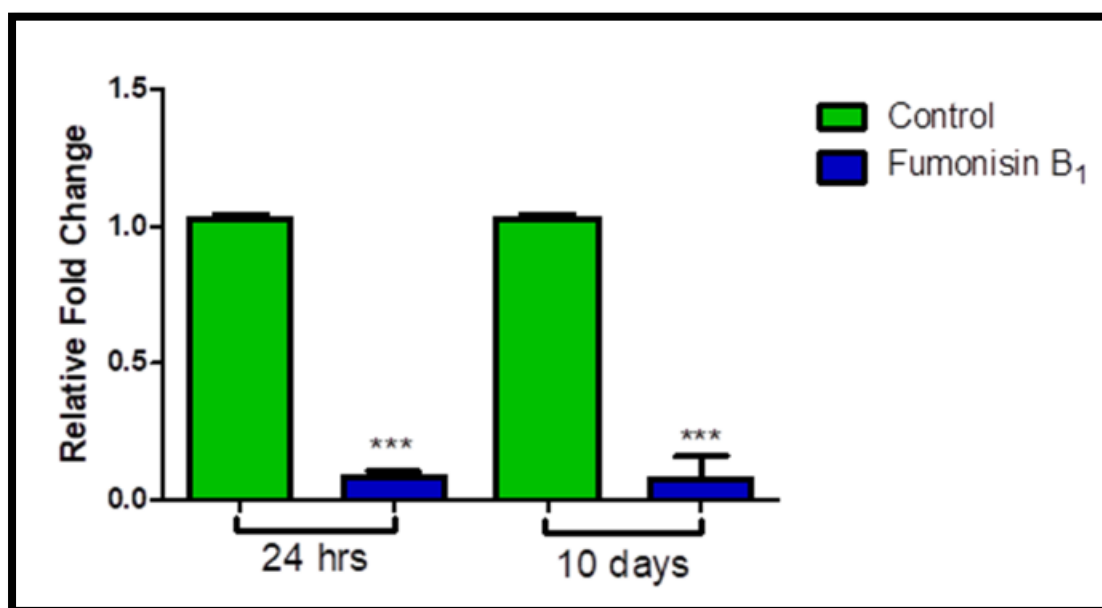


Figure 7: mRNA levels of *HO1* (24hrs: *** p < 0.0001; 10 days: *** p < 0.0001) in mice brain exposed to FB₁.

APPENDIX C

MiR-200a inhibits the Keap1-Nrf2 interaction, preventing Nrf2 from degradation by the proteasome. Using qPCR it was determined that FB₁ induced a significant increase in *miR-200a* levels in mice brain following acute (24hrs: *** $p < 0.0001$; Figure 8) and prolonged (10 days: ** $p = 0.0051$; Figure 8) exposure.

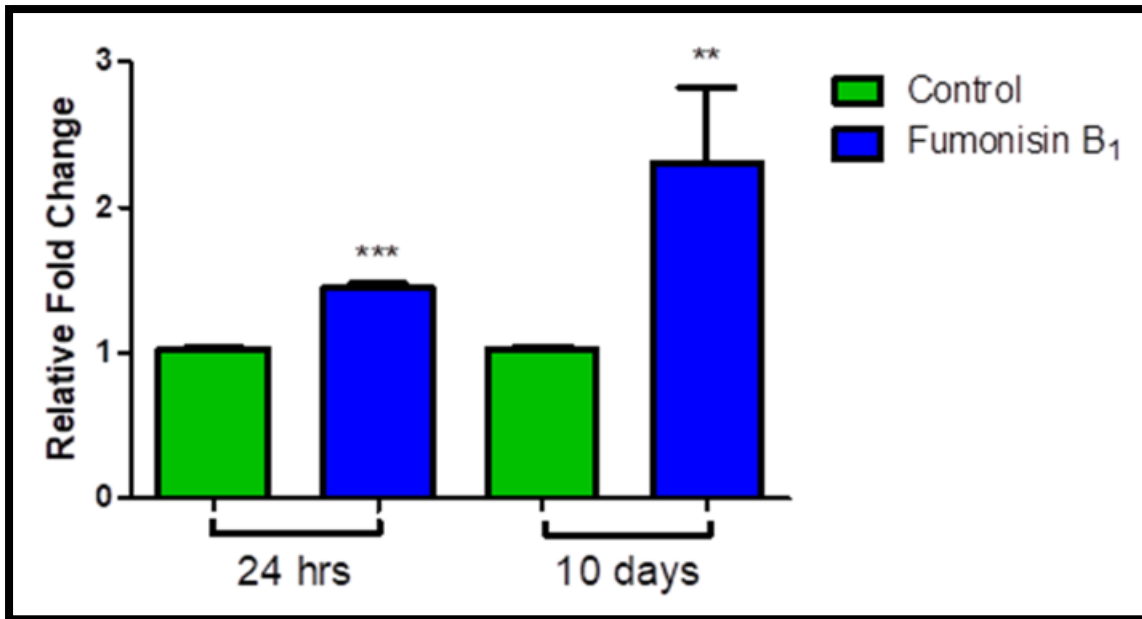


Figure 8: *MiR-200a* expression in C57BL/6 mice brain exposed to FB₁ for 24 hrs (*** $p < 0.0001$) and 10 days (** $p = 0.0051$).

APPENDIX D

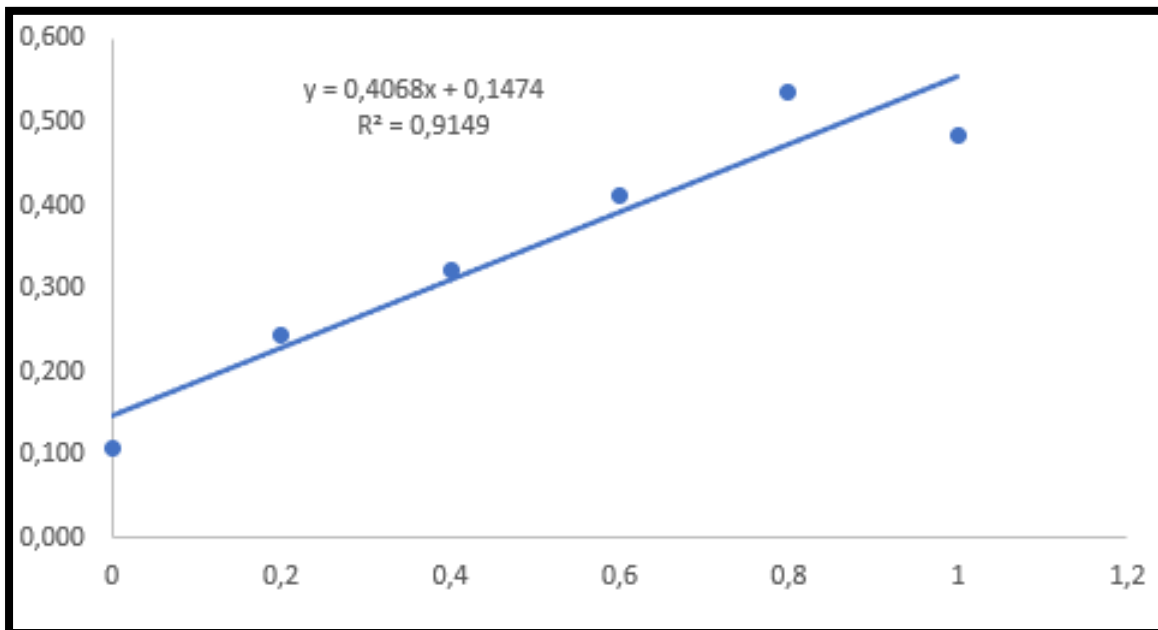


Figure 9: Standard curve displaying known concentrations of bovine serum albumin (BSA) used to determine the concentration of protein present in each sample